NEURAL CONTROL OF THE TONGUE IN THE COMMON MARMOSET

by

Paul Hage

A dissertation submitted to Johns Hopkins University in conformity with the requirements for the degree of Doctor of Philosophy

Baltimore, Maryland

June 2024

© 2024 Paul Hage

All rights reserved

Abstract

Flexible control of the tongue is critical across a wide range of human behaviors, including speech, mastication, respiration, and swallowing. Lingual movements exhibit dexterity, precision, and coordinated interactions with other oro-motor systems, making them an intriguing model for studying fine motor control. However, measuring tongue movements is challenging, and there is no established primate model for studying the neural basis of lingual control.

Here, we present the common marmoset as the first nonhuman primate model for the study of goal-directed lingual movements across two neuroscientific domains: the neuroeconomics of lingual control and the neurophysiology of lingual control by the cerebellum. Marmosets are capable of remarkable dexterity of their tongue, a skill they use in the wild to feed through extraction of sap from small holes made in trees. In this work, we leverage this ability in a foraging task in which marmosets are trained to produce goal-directed licks for food reward, while we record electrophysiological activity from the cerebellum.

In Chapter 2, we examine the effects of economic variables such as reward and effort on foraging-based decision-making and movement vigor of both saccades and licks. We found that when the acquisition of reward became effortful, the pupils constricted, the decisions exhibited delayed gratification, and the movements displayed reduced vigor. This coordinated response suggests that decisions and actions are part of a single control policy that aims to maximize a variable relevant to fitness: the capture rate.

In Chapter 3, we shift our focus to the cerebellum, examining the mechanism by which the principal cells of the cerebellar cortex, P-cells, contribute to control of the tongue. We identified lingual regions in lobule VI of the cerebellar vermis and recorded from P-cells as subjects performed goal-directed licks. We found that when P-cell simple spike activity was suppressed following a complex spike, licks exhibited endpoint

hypermetria. Further, we found that P-cell simple spike population firing rate responses exquisitely tracked lick deceleration, scaling with lick kinematics. These results suggest that P-cells contribute to the endpoint accuracy of a lick through enabling timely deceleration of movement.

Primary Reader and Advisor: Dr. Reza Shadmehr

Secondary Reader: Dr. David S. Zee

Thesis Committee: Dr. Reza Shadmehr, Dr. David S. Zee, Dr. Abigail Person

Acknowledgements

I must begin by thanking my PhD advisor, Dr. Reza Shadmehr. I can endlessly write about the important lessons that he has taught me about what it means to be a world-class scientist, a storyteller, and a deep, creative, and critical thinker. However, the most important lessons that I have learned from him, through his example, are about what it means to be human in science. His greatest qualities, beyond his intellect and ability to produce exceptional work, are kindness, compassion, and empathy. Thank you, Reza, for seeing potential in me and enabling me to chase my dreams.

I am incredibly grateful to my committee members: Dr. Abigail Person and Dr. David Zee. Besides being exceptional scientists who have produced a remarkable body of work throughout their careers, which our laboratory finds great inspiration in, they are uniquely kind, generous, and insightful human beings. On multiple occasions, they have demonstrated great generosity with their time by serving on the committees of various members of our laboratory. Thank you both for your support and for your roles that have uplifted me through graduate school.

Next, I must acknowledge my incredible lab mates. When I joined the laboratory in 2018, I was privileged to have role models in the senior students: Scott Albert, Tehrim Yoon, Simon Orozco, and Ehsan Sedaghat-Nejad. These students demonstrated to me what it meant to be exceptional graduate student scientists, and I spent my entire experience striving to follow in their footsteps. I must give a special thank you to Ehsan, who spent countless hours mentoring me and leading our efforts in building a marmoset lab. Further, I would like to acknowledge In Kyu Jang, Vivian Looi, Kaveh Karbasi, Jay Pi, and Tara Palin, who were incredible peers and instrumental in my success, as well as the success of our laboratory, through aiding in pioneering multiple aspects of our marmoset work.

Finally, I must acknowledge the next generation of students who joined after me: Mohammad Amin Fakharian, Alden Shoup, and Nazanin Rezaei, as well as our postdocs in the lab, Jafar Doostmohammadi and Solomon Muller. These individuals, through their incredible efforts, dramatically upgraded the quality of our work and made tremendous contributions to our training, surgical, and imaging protocols, to engineering our laboratory instruments, and in the generation of ideas and new, innovative behavioral paradigms. I must give a special thank you to Amin, who played an instrumental role in my projects, and who built the software infrastructure that is relied on by our entire lab. These individuals in many ways have become like family to me, sharing fond memories and demonstrating a level of talent that I can only strive to emulate.

Our lab's success would not have been possible without mentorship and support from members of Dr. Xiaoqin Wang's lab. Thank you to the incredible veterinary technicians: Jessica Lynch, Kayla Schonvisky, Sami Miller, Emma Easter, and Nia Bryan, who have been instrumental in maintaining the health of our precious animals and the state of their homes in the colony. Further, thank you to Wang lab scientists: Dr. Seth Koehler, Dr. Xiao-ping Liu, Dr. Xindong Song, Dr. Yueqi Guo, Dr. Chenggang Chen, Dr. Yang Zhang, Dr. Michael Osmanski, Dr. Jong Hoon Lee, and Dr. Xiaoqin Wang. Without their expertise in the marmoset model and their support early in the development of our marmoset lab, I and our laboratory would not be where we are today.

Next, I must thank my undergraduate research advisors, Dr. Sohini Roychowdhury and Dr. Pierre Mourad. Dr. Roychowdhury welcomed me to her group as a new transfer student to the University of Washington and, upon learning about my goal of attaining a PhD, paved my road to graduate school. She supported and mentored me through producing publications, presenting at conferences, and attaining scholarships. Dr. Pierre Mourad, through his work with his group, inspired in me a love for the study of motor control, eventually leading me to Reza's lab. Through his example, he taught me about the power of collaboration,

the importance of understanding patient experience, and the beauty of mentorship and teaching. Both individuals supported me in pursuing graduate school and continue to support me through every stage of my life.

Everything I have ever been able to achieve in my life, and any achievements to come in my future, are directly the result of the support, love, and example set by my parents, Denise and George. They are the hardest-working people I have ever come across in my life, who have dedicated their entire being to raising and helping facilitate the success of my sister and me. They always taught me that nothing is impossible and that if a particular goal has been achieved by another human being, then there is no reason that I cannot achieve it myself with heart, grit, and determination. Even in difficult times, they have offered me unrelenting support and drive to strive for things greater than I could have ever expected from myself. Thank you, Mum and Dad.

Finally, the single greatest thing to come out of my move to Baltimore for graduate school was meeting the love of my life, my best friend, and my partner through everything, my wife, Julie Shade. Together, we began by raising two beautiful dogs together, Kinjie and Echo, and more recently had our amazing son, Gabriel, who is the greatest source of joy, motivation, and love in our lives. No matter what I do in life or what circumstances we face, with you by my side and our family behind us, I will remain the happiest man on earth.

Dedication

This work is dedicated to my son, Gabriel. I hope it serves as an example that big goals can be achieved through hard work, discipline, and self-belief.

Table of Contents

Chapter 1 Introduction 1

Chapter 2 Effort cost of harvest affects decisions and movement vigor of marmosets during foraging 3

Chapter 2.1. Introduction 3

Chapter 2.2. Methods 5

Chapter 2.2.1. Data acquisition 5

Chapter 2.2.2. Data analysis 6

Chapter 2.2.3. Saccade and tongue vigor 7

Chapter 2.2.4. Model formulation 8

Chapter 2.2.5. Other models of utility 9

Chapter 2.2.6. Simulations 10

Chapter 2.2.7. Statistical analysis 10

Chapter 2.3. Results 11

Chapter 2.3.1. Theory and predictions 13

Chapter 2.3.2. Increased effort cost of harvest promoted work but reduces saccade vigor 17

Chapter 2.3.3. Increased effort cost of harvest reduced lick vigor 20

Chapter 2.3.4. Expectation of greater reward increased lick vigor 22

Chapter 2.3.5. Hunger promoted work and increased vigor 23

Chapter 2.3.6. Pupil size variations strongly correlated with changes in decisions and movements 25

Chapter 2.4. Discussion 26

Chapter 2.5. Supplementary Figures 30

Chapter 3 Control of goal-directed tongue movements by Purkinje cells of the cerebellum 31

Chapter 3.1. Introduction 31

Chapter 3.2. Methods 33

Chapter 3.2.1. Data acquisition 34

Chapter 3.2.2. Behavioral protocol 35

Chapter 3.2.3. Data analysis 36

Chapter 3.2.4. Computing the kinematic effects of CS-induced SS suppression 37

Chapter 3.3. Results 37

Chapter 3.3.1. CS-induced SS suppression produced overshooting of the tongue during protraction, and slowed return during retraction 39

Chapter 3.3.2. Perturbations scaled when pairs of P-cells were simultaneously suppressed 44

Chapter 3.3.3. The effects of SS suppression were consistent across P-cells regardless of their SS modulation 45

Chapter 3.3.4 The population SS response encoded the parameters of tongue kinematics 47

Chapter 3.3.5. Control studies 49
Chapter 3.4. Discussion 50
Chapter 3.5 Supplementary Figures 53
Chapter 4 Conclusions 56
Chapter 5 Bibliography 59
Chapter 6 Curriculum Vitae 68

List of Figures

Figure 2.1. Elements of a foraging task. 12

Figure 2.2. Theoretical results of an optimal control policy. 15

Figure 2.3. As the effort cost of harvest increased, subjects chose to work more trials, but slowed their movements. 18

Figure 2.4. As the effort cost of harvest increased, lick vigor declined, and the pupils constricted. 21

Figure 2.5. Relatively low body weight, potentially reflecting a greater valuation of reward, coincided with longer work periods and greater vigor. Pupil size correlated with both vigor and decisions. 25

Figure 3.1. Marmosets produced dexterous tongue movements during recordings from lobule VI of the cerebellar vermis. 35

Figure 3.2 CS rates increased with protrusion and decreased with retraction. 39

Figure 3.3. CS-induced SS suppression produced hypermetria during protraction and slowing during retraction. 41

Figure 3.4. Suppression of multiple P-cells scaled the perturbation to the tongue. 45

Figure 3.5. Effects of suppression remained consistent across P-cells regardless of SS modulation. 46

Figure 3.6. SS rates were greater for high vigor and long deceleration licks. However, little modulation was present during task irrelevant tongue movements. 49

Chapter 1 Introduction

The human tongue is a remarkably versatile organ crucial to a wide array of behaviors central to human experience. For instance, in speech, its rapid and precise changes in position and shape contribute to producing a vast range of sounds necessary for language expression. During eating, its role in intra-oral transport facilitates food manipulation to aid in chewing and initiate swallowing. In more automatic processes like respiration, its position and tone influence airway patency and breathing coordination.

Dysfunction in tongue control, often due to injury or neurodegenerative diseases, can profoundly affect quality of life. For example, patients with spinocerebellar ataxia frequently experience dysarthria, a motor-speech disorder leading to significant communication challenges and social isolation. Additionally, following a stroke, deficits in tongue control can lead to oral dysphagia, increasing the risk of malnutrition and life-threatening complications. Given its precision, dexterity, central role in basic human functions, and the severe impact of dysfunction in daily life, the tongue presents a fascinating model for studying the neural basis of fine motor control.

Currently, there is no established primate model for studying lingual movements, as the standard animal models typically involve rodents such as mice and rats engaged in simple behavioral paradigms like fluid licking. However, rodents are limited in their ability for flexible tongue control and have a less sophisticated nervous system. This gap poses challenges in extrapolating findings from rodent models to humans and limits discoveries related to more complex behaviors. In this study, we introduce the first primate model for studying complex lingual movements using the common marmoset (Callithrix jacchus).

Marmosets are gaining popularity as a non-human primate model for neuroscientific studies. They are small New World primates without known zoonotic diseases transferable to humans, making them safe and convenient to handle. Their size allows for the application of technologies and methods originally

designed for rodent models, while their more complex nervous system provides a richer subject for study. Behaviorally, they share important traits with humans: they are social and live in family units, vocalize with species-specific sound production, and use saccadic eye movements to explore their environments. Crucially, they are natural foragers with remarkable tongue dexterity. In the wild, they survive by locating and consuming plant exudates, such as tree sap, by gnawing small holes in trees with their incisors and skillfully extracting exudates using their tongues. These characteristics make them a compelling model for investigating the neural basis of both motor control and cognition.

In Chapter 2, we utilize the natural foraging abilities of two marmosets in a task where they perform saccades for food rewards and use goal-directed licks to consume rewards. We explore how economic variables such as reward and effort influence decisions to work or harvest, as well as the vigor of saccades and licks, while manipulating the effort cost associated with harvesting. Additionally, we measure pupil size as a proxy for internal state to gain insights into the brain's coupling of decision-making and movement vigor.

In Chapter 3, we take advantage of their small size to employ modern high-density recording probes to capture extracellular activity from lingual regions of the cerebellar vermis in three marmosets. The cerebellum is critical in facilitating smooth, accurate, and well-coordinated tongue movements, yet the mechanistic understanding of how it achieves this remains incomplete. We focus on P-cells, the principal neurons of the cerebellar cortex, and investigate how they contribute to the endpoint accuracy of licking movements.

Chapter 2 Effort cost of harvest affects decisions and movement vigor of marmosets during foraging

Our decisions are guided by how we perceive the value of an option, but this evaluation also affects how we move to acquire that option. Why should economic variables such as reward and effort alter the vigor of our movements? In theory, both the option that we choose and the vigor with which we move contribute to a measure of fitness in which the objective is to maximize rewards minus efforts, divided by time. To explore this idea, we engaged marmosets in a foraging task in which on each trial they decided whether to work by making saccades to visual targets, thus accumulating food, or to harvest by licking what they had earned. We varied the effort cost of harvest by moving the food tube with respect to the mouth. Theory predicted that the subjects should respond to the increased effort costs by choosing to work longer, stockpiling food before commencing harvest, but reduce their movement vigor to conserve energy. Indeed, in response to an increased effort cost of harvest, marmosets extended their work duration, but slowed their movements. These changes in decisions and movements coincided with changes in pupil size. As the effort cost of harvest declined, work duration decreased, the pupils dilated, and the vigor of licks and saccades increased. Thus, when acquisition of reward became effortful, the pupils constricted, the decisions exhibited delayed gratification, and the movements displayed reduced vigor. The following passages and figures derive from Hage et al., (2023).

Chapter 2.1. Introduction

During foraging, animals work to locate a food cache and then spend effort harvesting what they have found. As they forage, their decisions appear to maximize a measure that is relevant to fitness: the sum of rewards acquired, minus efforts expended, divided by time, termed the capture rate.[1–3] For example, a crow will spend effort extracting a clam from a sandy beach, but if the clam is small, it will abandon it because the additional time and effort required to extract the small reward --dropping it repeatedly from

a height onto rocks -- can be better spent finding a bigger prize.[4] In other words, if going to the bank entails waiting in a long line, one should go infrequently, but make each transaction a large amount. Intriguingly, reward expectation not only affects decisions, it also affects movements: we not only prefer the less effortful option, we also move vigorously to obtain it.[5,6] This modulation of movement vigor can be justified if we consider that movements require expenditure of time and energy, which discount the value of the promised reward.[7,8] Thus, from a theoretical framework, it seems rational that the brain should have a mechanism to coordinate control of decisions with control of movements so that both contribute to maximizing a measure of fitness.[9] To study this coordination, we designed a task in which marmosets decided how long to work before they harvested their food. On a given trial, they made a sequence of saccades to visual targets and received an increment of food as their reward. However, the increment was small, and its harvest was effortful, requiring inserting their tongue inside a small tube. Theory predicted that in order to maximize the capture rate, harvest should commence only when there was sufficient reward accumulated to justify the effort required for its extraction. Indeed, the subjects chose to work in order to stockpile food, and only then initiated their harvest. On some days the effort cost of harvest was low: the tube was placed close to the mouth. On other days the same amount of work, i.e., saccade trials, produced food that had a higher effort cost: the tube was located farther away. The theory made two interesting predictions: as the effort cost increased, the subjects should choose to work more trials, thus delaying their harvest so to stow more food, but reduce their movement vigor, thus saving energy. Indeed, when marmosets encountered an increased effort cost, they extended their work period, stockpiling food, but reduced their vigor, slowing their saccades during the work period, and slowing their licks during the harvest period. What might be a neural basis for this coordinated response of the decision-making and the motor control circuits? During the work and the harvest periods, momentary changes in pupil size closely tracked the changes in vigor: pupil dilation accompanied increases in vigor, while pupil constriction accompanied decreases in vigor. Remarkably, this was true

regardless of whether the movement that was being performed was a saccade, or a lick. Moreover, in response to the increased effort cost, the pupils exhibited a global change, constricting during both the work and the harvest periods. If we view the changes in pupil size as a proxy for activity in the brainstem noradrenergic circuits,[10] our results suggest that as these circuits respond to effort costs,[11] they alter computations in the brain regions that control decisions, delaying gratification and encouraging work, and the brain regions that control movements, promoting sloth and conserving energy.

Chapter 2.2. Methods

Behavioral and neurophysiological data were collected from two marmosets (*Callithrix Jacchus*, male and female, 350-390 g, subjects R and M, 6 years old). The neurophysiological data focused on the cerebellum and are described elsewhere.[12–14] Here, our focus is on the behavioral data.

The marmosets were born and raised in a colony that Prof. Xiaoqin Wang has maintained at the Johns Hopkins School of Medicine since 1996. The procedures on the marmosets were evaluated and approved by the Johns Hopkins University Animal Care and Use Committee in compliance with the guidelines of the United States National Institutes of Health.

Chapter 2.2.1. Data acquisition

Following recovery from head-post implantation surgery, the animals were trained to make saccades to visual targets and rewarded with a mixture of apple sauce and lab diet.[13] They were placed in a monkey chair and head-fixed while we presented visual targets on an LCD screen (Curved MSI 32” 144 Hz - model AG32CQ) and tracked both eyes at 1000 Hz using an EyeLink-1000 system (SR Research, USA). Timing of target presentation on the video screen was measured using a photo diode. Tongue movements were tracked with a 522 frame per second Sony IMX287 FLIR camera, with frames captured at 100 Hz.

Each trial began with a saccade to the center target followed by fixation for 200 ms, after which a primary target (0.5×0.5 deg square) appeared at one of 8 randomly selected directions at a distance of 5-6.5 deg.

Onset of the primary target coincided with presentation of a tone. As the animal made a saccade to the primary target, that target was erased, and a secondary target was presented at a distance of 2-2.5 deg, also at one of 8 randomly selected directions. The subject was rewarded if following the primary saccade it made a corrective saccade to the secondary target, landed within 1.5 deg radius of the target center, and maintained fixation for at least 200 ms. Onset of reward coincided with presentation of another distinct tone. Following an additional 150-250 ms period (uniform random distribution), the secondary target was erased, and the center target was displayed, indicating the onset of the next trial. Thus, a successful trial comprised of a sequence of 3 saccades: center, primary, and corrective, after which the subject received a small increment of food (0.015 mL).

The food was provided in two small tubes (4.4 mm diameter), one to the left and the other to the right of the animal (**Figure 2.1**A). A successful trial produced a food increment in one of the tubes and would continue to do so for 50-300 consecutive trials, then switch to the other tube. Because the food increment was small, the subjects naturally chose to work for a few consecutive trials, tracking the visual targets and allowing the food to accumulate, then stopped tracking and harvested the food via a licking bout. The licking bout typically included a sequence of 15-40 licks. The subjects did not work while harvesting. As a result, the behavior consisted of a work period (targeted saccades), followed by a harvest period (targeted licking), repeated hundreds of times per session.

The critical variables were the number of trials that the subject chose to perform before initiating harvest, the vigor of their saccades during the work period, and the vigor of their licks during the harvest period.

Chapter 2.2.2. Data analysis

All saccades, regardless of whether they were instructed by presentation of a visual target or not, were identified using a velocity threshold. Saccades to primary, secondary, and central targets were labeled as reward-relevant saccades, while all remaining saccades were labeled as task irrelevant.

We analyzed tongue movements using DeepLabCut.[15] Our network was trained on 89 video recordings of the subjects with 15-25 frames extracted and labeled from each recording. The network was built on the ResNet-152 pre-trained model, and then trained over 1.03×10 iterations with a batch size of 8, using a GeForce GTX 1080Ti graphics processing unit.[16] A Kalman filter was further applied to improve quality and smoothness of the tracking, and the output was analyzed in MATLAB to quantify varying lick events and kinematics.

We tracked the tongue tip and the edge of the food in the tube, along with control locations (nose position and tube edges). We tracked all licks, regardless of whether they were aimed toward the tube (reward seeking), or not (grooming). Reward seeking licks were further differentiated based on whether they aimed to enter the tube (inner-tube licks), hit the outer edge of the tube (outer-edge licks), or fell below the tube (under tube). If any of these licks successfully contacted the tube, we labeled that lick as a success (otherwise, a failed lick).

Pupil area was measured during a ±250 ms period centered at the onset of each reward-relevant saccade, and the onset of each lick. We then normalized the pupil measurements by representing it as a z-score with respect to the mean value for that session.

Chapter 2.2.3. Saccade and tongue vigor

We relied on previous work to define vigor of a movement.[5,17–19] Briefly, if the amplitude of a movement is x and the peak speed of that movement is v, then for each subject the relationship between the two variables can be described as:

$$v = \alpha\left(1 - \frac{1}{1+\beta x}\right) \qquad (3)$$

In the above expression, $\alpha,\beta \geq 0$ and are subject-specific parameters. For a movement with amplitude x, its vigor was defined as the ratio of the actual peak speed with respect to the expected value of its peak

speed, i.e., $\frac{v}{E[v(x)]}$. Expected value was computed by fitting Eq. (3) to all the data acquired across all sessions. When vigor is greater than 1, the movement had a peak velocity that was higher than the mean value associated with that amplitude.

Chapter 2.2.4. Model formulation

We chose a formulation of utility (Eq. 1) based on a normative approach that ecologists have used to understand the decisions that animals make regarding how far to travel for food, what mode of travel to use, and how long to stay before moving on to another reward opportunity.[4,20,21] In a typical formulation of the theory, the numerator represents the reward gained (in units of energy), minus the effort expended (also in units of energy), while the denominator represents the amount of time spent during that behavior. We represented this idea in Eq. (1) with saccades that produced reward accumulation, and licks that produced reward consumption. Thus, the utility that we aim to maximize is the rate of energy gained.

The specific functions that we used to represent the energy gained through reward acquisition, and the energy expended through effort expenditure, came either from experiment design, or from the measurements we have made in other experiments. We modeled reward accumulation as a linear rise in energy stored because successful saccades produced a linear increase in the food cache. We modeled harvesting of the food as a hyperbolic function of the number of licks to represent the fact that as the licking bout began, each successful lick depleted the food, and thus the first few licks produced a greater amount of food consumption than the last few licks. We modeled the effort cost of licking as a linear function of the number of licks.

A critical assumption that we made is that energy expended performing the saccade trials (which grew faster than linearly as a function of the number of trials attempted), grew faster than the time spent attempting those same trials (which grew linearly with the number of trials). This assumption is based on

the heuristic that the average rate of energy lost following a large number of attempted trials is greater than the average rate of energy lost following a small number of attempted trials.

The model's simplicity provided closed-form solutions across all parameter values, allowing us to make predictions without having to fit the model to the measured data. For example, for all parameter values that produce a real solution (as opposed to imaginary), the optimal number of saccade trials increases with the square root of the cost of licking. Thus, the basic prediction of the model is that to maximize the capture rate, regardless of parameter values, an increase in the effort required for harvest should be met with a greater willingness to work.

Chapter 2.2.5. Other models of utility

In composing our utility (Eq. 1), we chose to combine reward and effort additively. This is in contrast to other approaches in which effort discounts reward multiplicatively.[22–24] Our reasoning is that multiplicative interactions have the limitation that they are incompatible with the observation that reward invigorates movements.

To compare additive and multiplicative approaches, let us consider an arbitrary function u r that specifies how effort varies with movement duration *T*. Typically, this is a U-shaped function that describes energy expenditure as a function of movement duration, as in Shadmehr et al 2016.[8] In the case of multiplicative interaction between reward and effort, we can consider the following representation of utility:

$$J = \frac{\alpha}{1+T} U^{-1}(T) \qquad (4)$$

In the above formulation, reward a is discounted hyperbolically with time, and an increase in reward increases the utility of the action. The optimum movement vigor has the duration *T** that maximizes this utility. Notably, because increasing reward merely scales this utility, it has no effect on vigor. Thus, a utility

in which reward is multiplied by a function of effort generally fails to predict dependence of movement vigor on reward.

Chapter 2.2.6. Simulations

The optimal policy specifies the decisions and movements that for the effort cost defined in Eq. (2), maximizes the capture rate defined in Eq. (1). This policy selects the number of saccade trials n_s to perform during the work period, the number of licks n_l to perform during the harvest period, and the vigor of each lick, represented by the average duration of a lick T_l. To compute the optimal policy, we found the derivative of the capture rate with respect to each policy variable n_s, n_l, and T_l, then set each derivative equal to zero, producing three simultaneous nonlinear equations. In all three cases, we were able to solve for the relevant control variable analytically (see Mathematica notebook *simultatons.nb* for the derivations). We found that if the solution was a real number, then regardless of parameter values, an increase in *d* (distance of the tube to the mouth), the optimal policy produced an increase in n_s^*, decrease in n_L^*, and increase in T_L^*. Thus, the results illustrated in **Figure 2.2** are robust to changes in parameter values.

To generate the plots in **Figure 2.2**A, we used the following parameter values: $\alpha = 20$, $\beta_s = 0.5$, $\beta_L = 0.3$, $c_s = 0.5$, $T_s = 1$, $T_L = 0.2$, $c_L = 0.5$ (low effort), $c_L = 2.5$ (high effort). For the plots in **Figure 2.2**C-D, we used the same parameter values, but c_L was defined via Eq. (2). Thus, tube distance *d* varied, and T_L was unknown and was solved for. In Eq. (2), $k_L = 1$. In the simulations, to describe state of hunger, we set $\alpha = 20$ for a sated state and a= 25 for a hungry state.

Chapter 2.2.7. Statistical analysis

Hypothesis testing was performed using functions provided by the *MATLAB Statistics and Machine Learning Toolbox,* version R2021b. For t-tests, across the one-sample, paired-sample, and two-sample conditions, p values were computed using the *ttest* and *ttest2* functions with data that was combined

across sessions, separated by condition. For ANOVA tests, in the one-way condition, p values were computed using a nonparametric Kruskal-Wallis test, using the *kruskalwallis* function. In the 2-way condition, the *anovan* function was used to compute p values, accounting for an unbalanced design resulting from a varied number of samples across conditions. In both cases, like in the t-tests, data was combined across sessions, separated by condition. In the repeated measures condition, each session was treated as a subject with multiple repeated measures representing a given variable (i.e., lick vigor per lick in a harvest period). To fit a repeated measures model, the *fitrm* function was used, then analyzed using the *ranova* function. In all cases of repeated measures ANOVA, compound symmetry assumptions were tested using the Mauchly sphericity test with the *maulchy* function. In cases where the assumption was violated (Maulchy test $p < 0.05$), epsilon adjustments were used, with the *epsilon* function, to compute corrected p values (for $\varepsilon > .75$, use Huynh-Feldt p value and for $\varepsilon < .75$, use Greenhouse-Geisser p values). For correlation analyses, Pearson's correlation coefficient, r, and corresponding p values were computed using the *corrcoef* function.

Chapter 2.3. Results

We tracked the eyes and the tongue of head-fixed marmosets as they performed visually guided saccades in exchange for food (**Figure 2.1**A). Each successful trial consisted of 3 visually guided saccades, at the end of which we delivered an increment of food (a slurry mixture of apple sauce and monkey chow). Because the reward amount was small (0.015-0.02 mL), the subjects rarely harvested following a single successful trial. Rather, they worked for a few trials, allowing the food to accumulate, then initiated their harvest by licking (**Figure 2.1**B). The key variables were how many trials they chose to work before starting harvest, and how vigorously they moved their eyes and tongue during the work and the harvest periods.

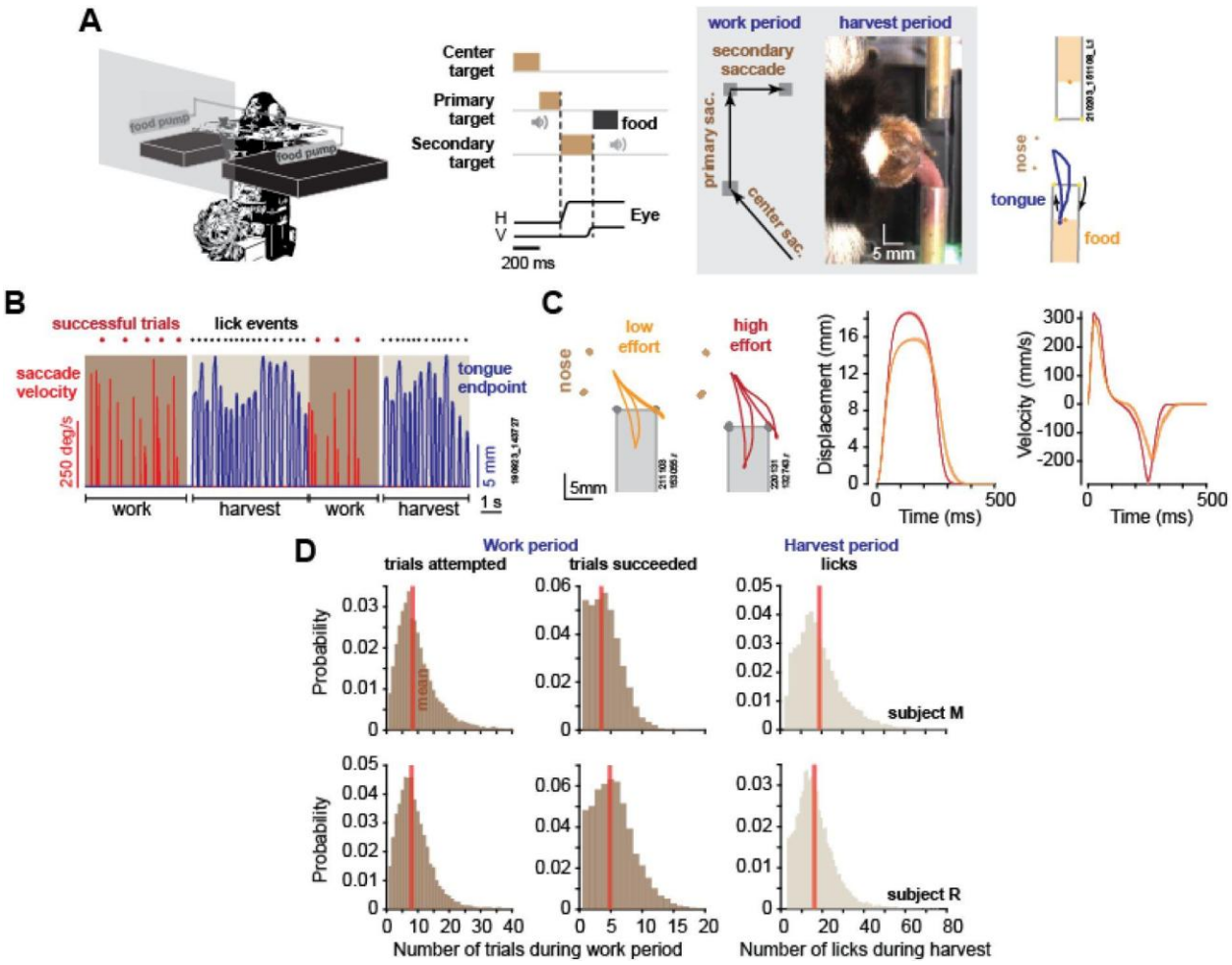


Figure 2.1. *Elements of a foraging task.*
A. During the work period, marmosets made a sequence of saccades to visual targets. A trial consisted of 3 consecutive saccades, at the end of which the subject was rewarded by a small increment of food. We tracked the eyes, the tongue, and the food. B. An example of two consecutive work-harvest periods, showing reward-relevant saccades (eye velocity) and tongue endpoint displacement with respect to the mouth. C. Data for two sessions, one where the tube was placed close to the mouth (orange trace), and one where it was placed farther away (red trace). Two types of licks are shown: inner-tube licks, and outer-tube licks. Depending on food location, both types of licks can contact the food. Data on the right two panels show endpoint displacement and velocity of the tongue during inner-tube licks. Error bars are SEM. D. During the work period, the subjects attempted about 8 trials on average, succeeding in 4-5 trials before starting harvest, and then licked about 18 times to extract the food.

Over the course of 2.5 years, we recorded 56 sessions in subject M (29 months) and 56 sessions in subject R (23 months). A typical work period lasted about 10 seconds, during which the subjects attempted ~8 trials, and succeeded in 4-5 trials (**Figure 2.1**D) (a successful trial was when all three saccades were within 1.25 of the center of each target). The work period ended when the subject decided to stop tracking the targets and instead initiated harvest, which lasted about 6 seconds, resulting in 16-18 licks. Subject M completed an average of 909.5 ± 61 successful trials per session (mean ± SEM), producing an average of

241 ± 13.9 work-harvest pairs, and subject R completed an average of 1431 ± 65 successful trials, producing an average of 263 ± 8.9 work-harvest pairs.

We delivered food via either the left or the right tube for 50-300 consecutive trials, and then switched tubes. We tracked the motion of the tongue using DeepLabCut,[15] as shown for a typical session in **Figure 2.1**B. The licks required precision because the tube was just large enough (4.4 mm diameter) to allow the tongue to penetrate. As a result, about 30% of the of the reward-seeking licks were successful and contacted food (30±1.6% for subject M, 28±2.5% for subject R), as shown in Supporting Information Video 1. Example of licks that failed to contact food are shown in Supporting Information Video 2, Video 3, and Video 4.

Chapter 2.3.1. Theory and predictions

During the decision-making part of the task, the brain explicitly determined how long to work before initiating harvest. During the work and the harvest periods, the brain implicitly controlled the vigor of movements. We imagined that these two forms of behavior were not independent, but rather coordinated via a control policy that maximized a single utility: the sum of rewards acquired, minus efforts expended, divided by time, termed the capture rate. We chose this formulation because it presents a normative approach that ecologists have used to understand the decisions that animals make regarding how far to travel for food, what mode of travel to use, and how long to stay before moving on to another patch.[4,20,21]

During a work period, our subjects decided to complete a number of saccade trials n_s, a fraction β_s of which were successful, earning food increment α, but expended effort c_s that consumed time T_s for each trial. They then stopped working and initiated harvest, producing a number of licks n_l, a fraction β_l of which succeeded, thus expending effort c_l and consuming time T_l for each lick. These actions produced the following capture rate:

$$J = \frac{\alpha\beta_s n_s\left(1 - \frac{1}{1+\beta_l n_l}\right) - n_l c_l - n_s^2 c_s}{n_l T_l + n_s T_s} \quad (1)$$

In the numerator of Eq. (1), the first term represents the fact that the food cache increased linearly with successful trials and was then consumed gradually with successful licks. The second term represents the effort expenditure of licking, and the third term represents the effort expenditure of working. Notably, the effort expenditure of work, $n_s^2 c_s$, grows faster than linearly as a function of trials. This nonlinearity is essential to reflect the idea that following a long work period, the capture rate must be more negative than following a short work period (i.e., more work trials produce a greater reduction in utility).

A control policy describes how long to work and harvest, and an optimal policy produces periods of working and harvesting, n_s^*, n_l^*, that maximize Eq. (1). A closed-form solution for the optimal policy can be obtained (*Mathematica* notebook simulations.nb) and **Figure 2.2**A provides an example. As the work period concludes and the harvest period begins (n_l = 0), the capture rate is negative. This reflects the fact that the subject has performed a few trials and stockpiled food, thus expended effort but has not been rewarded yet. The capture rate rises when licking commences. Critically, the peak capture rate is not an increasing function of the work period. Rather, there is an optimal work period (n_s^*, red trace, **Figure 2.2**A) associated with a given effort cost of licking c_l. If we now move the tube away from the mouth, that is, increase the effort cost of licking c_l, the peak of the capture rate shifts and the optimal work period changes: the proper response to an increased effort cost of licking is to work longer, stowing more food before commencing harvest.

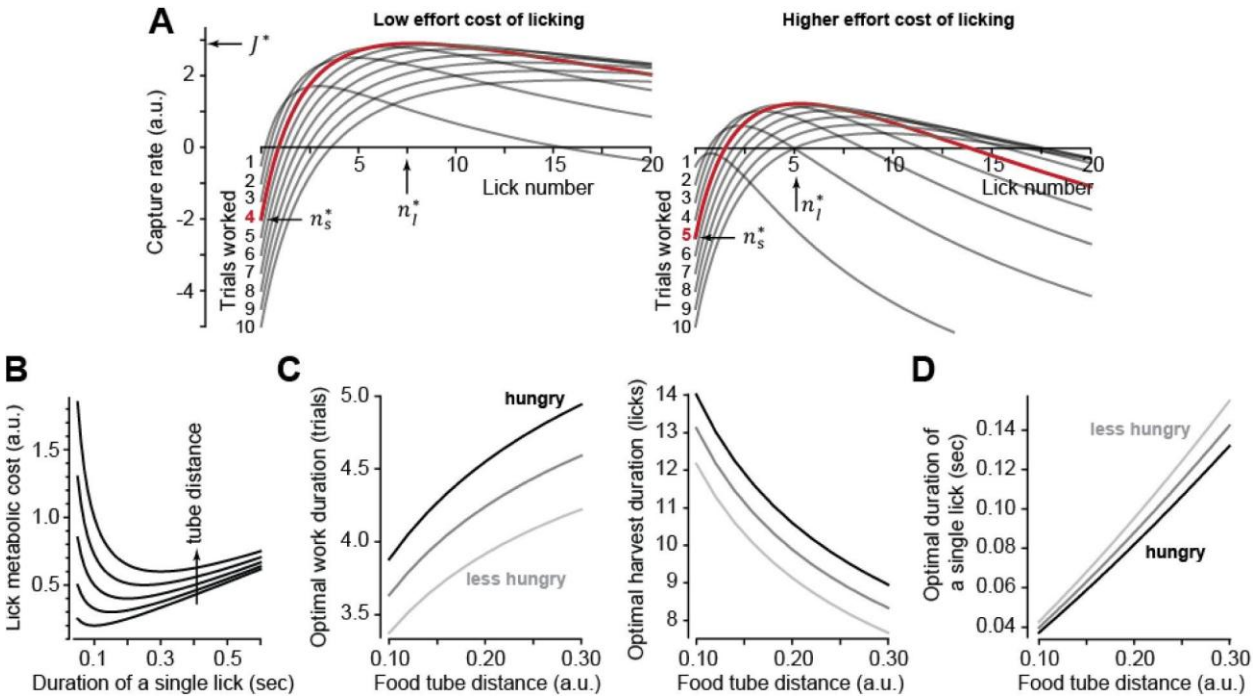


Figure 2.2. *Theoretical results of an optimal control policy.*
A. Capture rate (Eq. 1) is plotted during the harvest period as a function of lick number following various number of work trials. When the effort cost of licking is low (left plot,), the optimal work period is (red trace). When the effort cost is higher (right plot,), it is best to work longer before initiating harvest. B. The metabolic cost of licking (Eq. 2) is minimized when a lick has a specific duration. Tube distance varied from 0.1 to 0.3. Optimal duration that minimizes lick cost grows linearly with tube distance. C. Optimal number of work trials and licks as a function food tube distance. As the effort cost of harvest increases, one should respond by working longer, delaying harvest. D. Optimal lick duration as a function of food tube distance. The lick duration that maximizes the capture rate is smaller than the one that minimizes the lick metabolic cost (B). That is, it is worthwhile moving vigorously to acquire reward. However, it grows faster than linearly as a function of tube distance. Thus, as the tube moves farther, it is best to reduce lick vigor. Hunger, modeled as increased value of reward, should promote work and increase vigor, while effort cost of harvest (tube distance) should promote work but reduce vigor. Parameter values for all simulations: (low food value, less hunger), (high food value, hungry)., the higher cost of licking inevitably reduces the maximum capture rate (A). This should impact movement vigor: animals tend to respond to a reduced capture rate by slowing their movements (9), which can be viewed as an effective way to save energy (8). To incorporate vigor into the capture rate, we tried to define the effort cost of a single lick cl in terms of its energetic cost, a relationship that is currently unknown. Fortunately, other movements provide a clue: the energetic cost of reaching

Notably,[8,25] as well as the energetic cost of walking,[26,27] are both concave upward functions of the movement's duration. That is, from an energetic standpoint, there is a reach speed, and a walking speed, that minimizes the cost of each type of movement. We generalized these empirical observations to licking and assumed that the energetic cost of a single lick was a concave upward function of its duration:

$$c_l(T_l) = \frac{d^2}{T_l} + kT_l \qquad (2)$$

In Eq. (2), the lick is aimed at a tube located at distance *d*, and has a duration T_l. The parameter *k* describes the rate with which the cost grows as a function of duration. For example, the lick duration that minimizes the energetic cost is $d/\sqrt{k}$. Thus, for an energetically optimal lick, duration grows linearly with tube distance (**Figure 2.2**B). However, our objective is not to minimize the cost of licking, but to maximize the capture rate. To do so, we insert Eq. (2) into Eq. (1) and find the optimal policy (n_s^*, n_l^*, T_l^*), which now depends on the distance of the food tube to the mouth.

The theory predicts that to maximize the capture rate (Eq. 1), the response to an increased effort cost of harvest (i.e., tube distance) should be as follows: n_s^* should increase (**Figure 2.2**C), n_l^* should decrease (**Figure 2.2**C), and T_l^* should increase (**Figure 2.2**D). Notably, the rate of increase in T_l^* as a function of tube distance is faster than linear, while from an energetic point of view (Eq. 2), increase in distance should produce a linear increase in lick duration. Thus, as the harvest becomes more effortful, the subject should work longer to stockpile food, but move slower to save energy.

To test our theory further, we thought it useful to have a way to alter decisions in one direction (say work longer) but change movement vigor in the opposite direction (move faster). In theory, this is possible: if the subject is hungry (darker lines in **Figure 2.2**C-D), i.e., the reward is more valuable, then they should again work longer before initiating harvest. Paradoxically, they should also move faster.

In summary, if decisions and actions are coordinated via a policy that aims to maximize the capture rate, then in response to an increased cost of harvest, one should work longer, but move with reduced vigor. In response to an increased reward value, as in hunger, one should also work longer, but now move with increased vigor.

Chapter 2.3.2. Increased effort cost of harvest promoted work but reduces saccade vigor

To vary the effort cost of harvest, we altered the tube distance to the mouth (but kept it constant during each session). Varying tube distance affected the decisions of the subjects: when the tube was placed farther, they chose to work longer before starting harvest (**Figure 2.3**A, left subplot): they attempted more trials during each work period (ANOVA, subject M: $F(2,7908)=41.5$ $p=5.2\times10^{-25}$, subject R: $F(2,10948)=88.2$ $p=7\times10^{-50}$), and produced more successful trials per work period (ANOVA, subject M: $F(2,7908)=63$ $p=2.8\times10^{-24}$, subject R: $F(2,10948)=163$ $p<10^{-50}$). This policy of delayed gratification was present throughout the recording session (**Figure 2.3**A, middle plot). That is, when the harvest required more effort, the subjects worked longer to stockpile more food before initiating their harvest (**Figure 2.3**A, right plot, effect of tube distance on food cached: subject M: $F(2,9566)=176$ $p<10^{-50}$, subject R: $F(2,8907)=204$ $p<10^{-50}$).

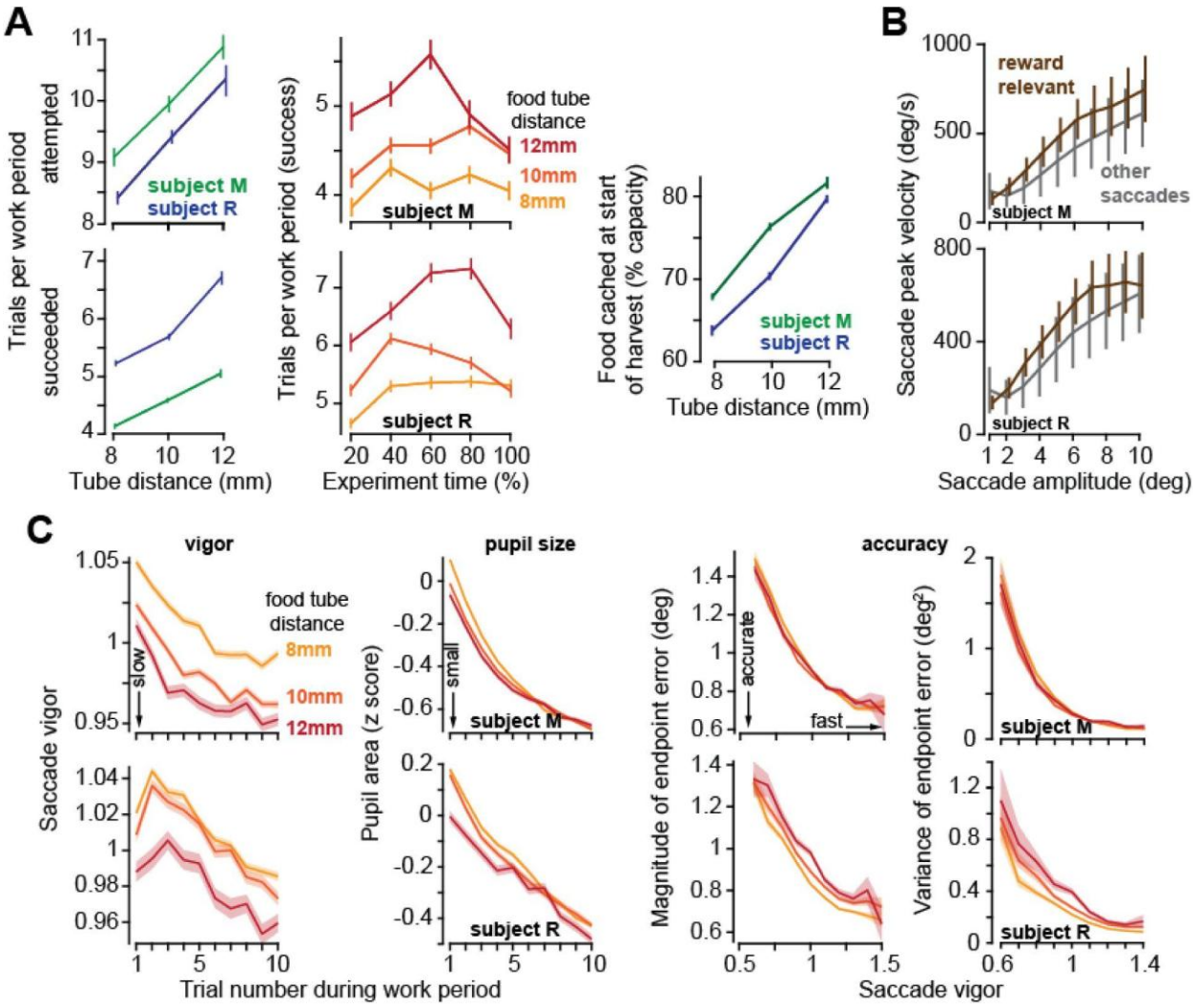


Figure 2.3. *As the effort cost of harvest increased, subjects chose to work more trials, but slowed their movements. A. Left: the number of trials attempted and succeeded per work period as a function of tube distance. Middle: successful trials per work period as a function of time during the recording session. Tube distance is with respect to a marker on the nose. Right: food available in the tube at the start of the harvest. B. Peak saccade velocity as a function of amplitude for reward-relevant and other saccades. C. Vigor of reward relevant saccades as a function of trial number during the work period. Saccade vigor was greater when the tube was closer. Pupil size is quantified during the same work periods. Accuracy is quantified as the magnitude of the saccade's endpoint error vector (with respect to the target) and the variance of that error vector (determinant of the variance-covariance matrix), plotted as a function of the vigor of the saccade (bin size=0.05 vigor units). Error bars are SEM.*

During the work period the subjects made saccades to visual targets and accumulated their food. They also made saccades that were not toward visual targets and thus were not eligible for reward. For each animal we computed the relationship between peak saccade velocity and saccade amplitude across all sessions and then calculated the vigor of each saccade: defined as the ratio of the actual peak velocity with respect to the expected peak velocity for that amplitude.[18,19] For example, a saccade that exhibited

a vigor of 1.10 had a peak velocity that was 10% greater than the average peak velocity of the saccades of that amplitude for that subject. As expected, the reward-relevant saccades, i.e., saccades made to visual targets (primary, corrective, and center saccades) were more vigorous than other saccades (**Figure 2.3**B, 2-way ANOVA, effect of saccade type, subject M: $F(1,391459)=7248$ $p<10^{-50}$, subject R: $F(1,355839)=13641$ $p<10^{-50}$).

As a work period began, the reward-relevant saccades exhibited high vigor, but then trial-by-trial, this vigor declined, reaching a low vigor value just before the work period ended (**Figure 2.3**C vigor). Remarkably, on days in which the tube was placed farther, saccade vigor was lower (RMANOVA, effect of tube distance, subject M: $F(2,59033)=224$ $p<10^{-50}$, subject R: $F(2,50103)=75.51$ $p=1.8\times10^{-33}$). Thus, increasing the effort cost of extracting food during the harvest period reduced saccade vigor during the work period.

By definition, a more vigorous saccade had a greater peak velocity. This might imply that high vigor saccades should suffer from inaccuracy due to signal dependent noise.[28] However, we observed the opposite tendency: as saccade vigor increased, both the magnitude and the variance of the endpoint error decreased (**Figure 2.3**C, 2-way ANOVA, effect of vigor on error magnitude, subject M: $F(8,59046)=480$ $p<10^{-50}$, subject R: $F(8,50184)=252$ $p<10^{-50}$, effect of vigor on error variance, subject M: $F(8,2673)=18200$ $p<10^{-50}$, subject R: $F(8,2673)=4170$ $p<10^{-50}$). That is, reducing the effort costs of harvest not only promoted vigor, it also facilitated accuracy.[29]

Cognitive signals such as effort and reward are associated with changes in pupil size,[10] as well as transient activation of brainstem neuromodulatory circuits in locus coeruleus.[11] We wondered if the changes in tube position altered the output of these neuromodulatory circuits, as inferred via pupil size. For each reward-relevant saccade, we measured the pupil size during a ±250 ms window centered on saccade

onset, and then normalized this measure based on the distribution of pupil sizes that we had measured during the entire recording for that session in that subject, resulting in a z-score.

At the onset of each work period the pupils were dilated, but as the subjects performed more trials, the pupils constricted, exhibiting a trial-by-trial reduction that paralleled the changes in saccade vigor (**Figure 2.3**C). Notably, the effort cost of harvest affected pupil size: during the work period the pupils were more dilated if the tube was placed closer to the mouth (**Figure 2.3**C, RMANOVA, effect of tube distance, subject M: $F(2,60502)=20$ $p=2\times10^{-9}$, subject R: $F(2,50431)=23.8$ $p=4.9\times10^{-11}$). That is, when the effort cost of harvest was lower, the pupils dilated, and the saccades were invigorated.

In summary, when we increased the effort cost of harvest, both the movements and the decisions changed: the pupils constricted and the movements slowed, but they chose to work more trials before initiating harvest.

Chapter 2.3.3. Increased effort cost of harvest reduced lick vigor

The work period ended when the subject chose to stop tracking the target and initiated harvest via a licking bout. As in saccades, we defined lick vigor via the ratio of the actual peak velocity of the lick with respect to the expected velocity for that lick amplitude. As amplitude increased, lick peak velocity increased during both protraction and retraction (**Figure 2.4**A). Some of the licks were reward seeking and directed toward the tube, while others were grooming licks, cleaning the tongue and the area around the mouth (Supporting Information Video 5). Reward-seeking licks were more vigorous than grooming licks (2-way ANOVA, effect of lick type, protraction, subject M: $F(1,272233)=66$ $p=4.5\times10^{-16}$, subject R: $F(1,229052)=698$ $p<10^{-50}$), and retraction was more vigorous than protraction (reward seeking licks, retraction vs. protraction, subject M: $t(241145)=532$ $p<10^{-50}$, subject R: $t(213674)=665$ $p<10^{-50}$).

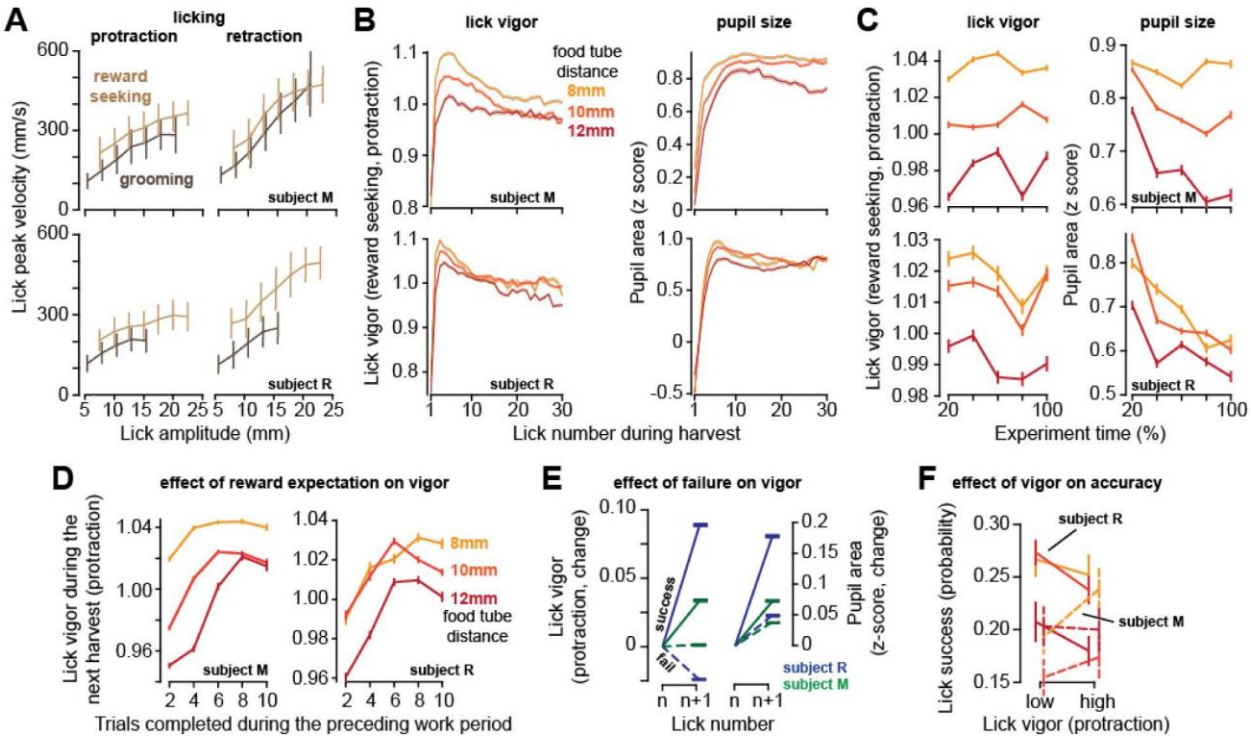


Figure 2.4. *As the effort cost of harvest increased, lick vigor declined, and the pupils constricted.*
A. Peak speed of reward-seeking and grooming licks during protraction and retraction as a function of lick amplitude. B. Vigor of reward seeking licks (protraction) and pupil size as a function of lick number during harvest at various tube distances. C. Lick vigor and pupil size as a function of time during the entire recording session. Line colors depict tube distance as in part B. D. Average lick vigor and pupil size during a harvest as a function of number of trials successfully completed in the previous work period. Lick vigor and pupil size were greater when more food had been stored. E. Following a successful lick (contact with food), the next lick was more vigorous, and pupils dilated. Following a failed lick, the next lick was slowed, and pupils were less dilated. F. We observed no consistent effect of lick vigor on lick accuracy across subjects or across tube distances. Error bars are SEM.

As the harvest began, the first lick was very low vigor, but lick after lick, the movements gathered velocity, reaching peak vigor by the 3rd or the 4th lick (**Figure 2.4**B). As the harvest continued, lick vigor gradually declined. Like saccades, licks had a lower vigor in sessions in which the tube was placed farther from the mouth (RMANOVA, effect of tube distance, subject M: $F(2,59033)=222.5$ $p<10^{-50}$, subject R: $F(2,133502)=224$ $p<10^{-50}$), and this pattern was present during the entire recording session (**Figure 2.4**C, left subplot). Thus, an increased effort cost of harvest promoted sloth: reduced vigor of saccades during the work period, and reduced vigor of licks during the harvest period.

For each reward seeking lick, we measured pupil size during a ±250ms window centered on the moment of peak tongue displacement. During licking, the pupil size changed with a pattern that closely paralleled

lick vigor: as the harvest began, pupil size was small, but it rapidly increased during the early licks, then gradually declined as the harvest continued (**Figure 2.4**B, right subplot). Importantly, the pupils were more dilated in sessions in which the tube was closer to the mouth (**Figure 2.4**C, right subplot, effect of tube distance, subject M: $F(2,166742)=583$ $p<10^{-50}$, subject R: $F(2,130493)=118$ $p<10^{-50}$). As a result, when the effort cost of reward increased, the pupils constricted, and the vigor of both saccades and licks decreased.

While the theory predicted that moving the tube farther would result in a longer work period and reduced movement vigor, it also predicted that the subjects would reduce their harvest duration (reduced licks, **Figure 2.4**C). That is, it predicted that the subjects would work longer, stowing more food, but leave more of it behind. This last prediction did not agree with our data (see Discussion). For Subject R, the number of licks were approximately the same across the various tube distances, and for Subject M the number of licks increased with tube distance (**Supplementary Figure 2.1**).

In summary, within a harvest period, lick vigor rapidly increased and then gradually declined. Simultaneous with the changes in vigor, the pupils rapidly dilated and then gradually constricted. In sessions where the tube was placed farther from the mouth, the licks had lower vigor, and the pupils were more constricted.

Chapter 2.3.4. Expectation of greater reward increased lick vigor

As the subject worked, they accumulated food, thus increasing the magnitude of the available reward. To check whether reward magnitude affected movement vigor, for each tube distance we computed the average lick vigor during the harvest as a function of the number of trials completed in the preceding work period. We found that when the work period had included many completed trials, then the movements in the ensuing harvest period were more vigorous (**Figure 2.4**D, 2-way ANOVA, effect of trials, subject M: $F(4, 164242)=353$ $p<10^{-50}$, subject R: $F(4,123411)=152$ $p<10^{-50}$). Thus, the licks were invigorated by the amount of food that awaited harvest.

Because the tube was small, many of the licks missed their goal and failed to contact the food. The success or failure of a lick affected both the vigor of the subsequent lick, and the change in the size of the pupil. Following a successful lick there was a large increase in lick vigor (**Figure 2.4**E, subject M: $t(85182)=40$ $p<10^{-50}$, subject R: $t(81378)=104$ $p<10^{-50}$), and a large increase in pupil size (subject M: $F(84969)=57$ $p<10^{-50}$, subject R: $t(80318)=94$ $p<10^{-50}$). In contrast, following a failed lick the subjects either reduced or did not increase their lick vigor (**Figure 2.4**E, subject M: $t(114159)=0.88$ $p=0.37$, subject R: $t(97164)=-44$ $p<10^{-50}$). This failure also produced a smaller increase in pupil size (comparison to successful lick, two sample t-test, subject M: $t(198722)=14.8$ $p=4.3\times10^{-50}$, subject R: $t(176044)=53$ $p<10^{-50}$). Thus, a single successful lick led to acquisition of reward, which then was followed by a relatively large increase in pupil size, and an invigorated subsequent lick.

For saccades we had found that increased vigor was associated with greater accuracy. To quantify the relationship between lick vigor and accuracy, for each tube distance we labeled each reward seeking lick as being high or low vigor. For subject M, high vigor licks tended to be more successful, but this was not the case for subject R (**Figure 2.4**F). Moreover, tube distance did not produce a consistent effect on lick success.

In summary, the subject licked more vigorously following a long work period in which they had accumulated more reward. Moreover, when a lick was successful in acquiring reward, they increased the vigor of the subsequent lick.

Chapter 2.3.5. Hunger promoted work and increased vigor

Our theory predicted that it should be possible to change decisions in one direction (say work longer), while altering movement vigor in the opposite direction (move faster). An increase in the subjective value of reward, as might occur when the subject is hungry, should have two effects: increase the number of trials that the subject chooses to perform before commencing harvest, and increase movement vigor.

We did not explicitly manipulate the weight of the subjects. Indeed, to maintain their health, we strived to keep their weights constant during the roughly 2.5-year period of these experiments. However, there was natural variability, which allowed us to test the predictions of the theory.

We found that when their weight was lower than average, the subjects chose to work a greater number of trials before commencing harvest (**Figure 2.5**A, two sample t-test, subject M: $t(11052)=7.9$ $p=3.4\times10^{-25}$, subject M: $t(12549)=10.1$ $p=9.3\times10^{-24}$). This result was similar to the effect that we had seen when the effort cost of harvest was increased. However, the theory had predicted that the effect on vigor should be in the opposite direction: if hunger increased reward valuation, then one should speed the movements and hasten food acquisition. Notably, weight did not have a consistent effect on saccade vigor across the two subjects (**Figure 2.5**A), yet during the harvest, both subjects licked with greater vigor when their weight was lower (**Figure 2.5**A, subject M: $t(219752)=88$ $p<10^{-50}$, subject R: $t(205163)=22$ $p<10^{-50}$).

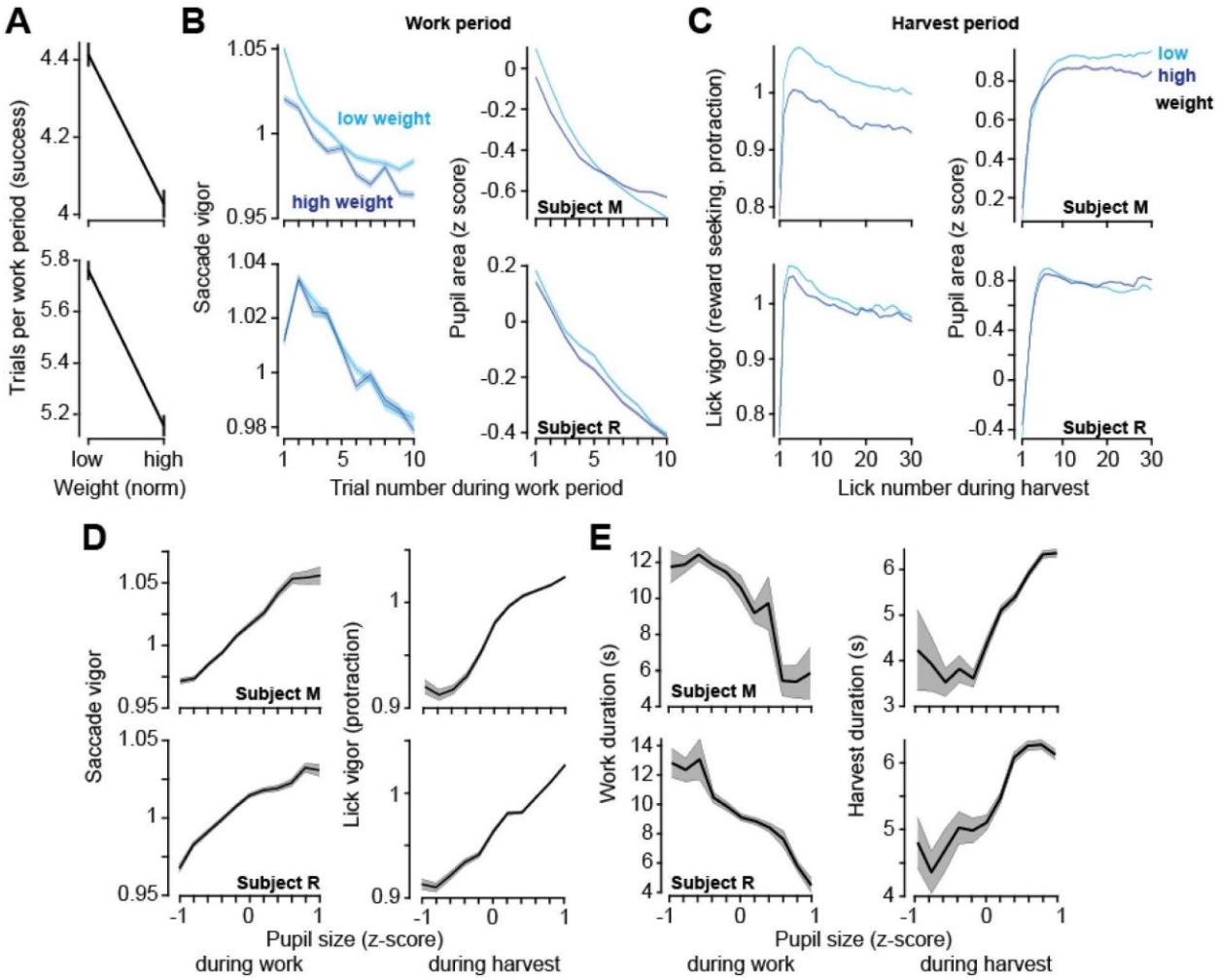


Figure 2.5. *Relatively low body weight, potentially reflecting a greater valuation of reward, coincided with longer work periods and greater vigor. Pupil size correlated with both vigor and decisions.*
A. Trials successfully completed during a work period as a function of normalized body weight at the start of the session. B. Left: saccade vigor as a function of trial number for low and high body weights. Right: pupil size during the same saccades. C. Left: lick vigor as a function of lick number during the harvest period. Right: pupil size during the same licks. D. Saccade vigor during the work period, and lick vigor during the harvest period, as a function of pupil size. E. Work duration and harvest duration as a function of pupil size. Error bars are SEM.

Thus, while both the effort cost of reward and hunger promoted greater work, effort promoted sloth while hunger promoted lick vigor.

Chapter 2.3.6. Pupil size variations strongly correlated with changes in decisions and movements

Finally, we considered the data across both the work and the harvest periods and asked how well movement vigor tracked pupil size. The results demonstrated that in both the work and the harvest

periods, for both saccades and licks, an increase in pupil size was associated with an increase in vigor (**Figure 2.5**B, reward-relevant saccades, subject M: r=0.989 $p=7.7\times10^{-9}$, subject R: r=0.97 $p=7.1\times10^{-7}$, reward-seeking protraction licks, subject M: r=0.969 $p=9.8\times10^{-7}$, subject R: r=0.989 $p=6.3\times10^{-9}$). Moreover, when the pupil was dilated, the work periods tended to be shorter (**Figure 2.5**C, subject M: r=-0.90 p=0.00014, subject R: r=-0.97 $p=6.3\times10^{-7}$), while harvest durations tended to be longer (**Figure 2.5**C, subject M: r=0.894 p=0.00021, subject R: r=0.935 $p=2.4\times10^{-5}$). Thus, pupil dilation was associated with choosing to work less, while moving faster.

Chapter 2.4. Discussion

What we choose to do is the purview of the decision-making circuits of our brain, while the implicit vigor with which we perform that action is the concern of the motor-control circuits. From a theoretical perspective,[17] our brain should coordinate these two forms of behavior because both the act that we select, and its vigor, dictate expenditure of time and energy, contributing to a capture rate that affects longevity and fecundity.[30] Does the brain coordinate decisions and movements to maximize a capture rate? If so, how might the brain accomplish this coordination?

Here, we designed a foraging task in which marmosets worked by making saccades, accumulating food for each successful trial, then stopped working and harvested their cache by licking. On every trial they decided whether to work, or to harvest. Their decision was carried out by the motor system, producing either a visually guided saccade, or a lick, each exhibiting a particular vigor. The theory predicted that to maximize the capture rate, the appropriate response to an increased effort cost of harvest was to do two things: work longer to cache more food but reduce vigor to conserve energy.

We varied the effort costs by moving the food tube with respect to the mouth. This changed the effort cost of harvest but not the effort cost of work. The subjects responded by altering how they worked as well as how they harvested. When the harvest was more effortful, they performed more saccade trials to

stockpile food. They also slowed their movements, reducing saccade velocity during the work period, and reducing lick velocity during the harvest period. Notably, the most vigorous saccades were also the most accurate: as saccade vigor increased, so did endpoint accuracy.

The theory made a second prediction: as the value of reward increased, the subjects should again choose to work a longer period before initiating harvest, but unlike the effort costs, now respond by moving more vigorously. We did not directly manipulate the subjective value of reward, but rather relied on the natural fluctuations in body weight and assumed that when their weight was low, the subjects were hungrier for reward. Indeed, when their weight was low, the subjects again chose to work longer, but now elevated their vigor during the harvest period.

Finally, we quantified the effect of reward magnitude on vigor. Within a session, lick vigor increased robustly as a function of the number of trials completed in the preceding work period. Thus, the licks were invigorated by the amount of food that awaited harvest.

Notably, some of the predictions of the theory did not agree with the experimental data. An increased effort cost did not accompany a reduction in the duration of harvest, and hunger did not increase saccade vigor robustly. Indeed, earlier experiments have shown that if the effort cost of harvest increases, animals who expend the effort will then linger longer to harvest more of the reward that they have earned.[2] This mismatch between observed behavior and theory highlights some of the limitations of our formulation. For example, our capture rate reflected a single work-harvest period, rather than a long sequence. Moreover, the capture rate did not consider the fact that the food tube had finite capacity, beyond which the food would fall and be wasted. This constraint would discourage a policy of working more but harvesting less. Finally, if we assume that a reduced body weight is a proxy for increased subjective value of reward, it is notable that we observed a robust effect on vigor of licks, but not saccades. A more realistic capture rate formulation awaits simulations, possibly one that describes capture rate not as the ratio of

two sums (sum of gains and losses with respect to sum of time), but rather the expected value of the ratio of each gain and loss with respect to time.[31,32]

A shortcoming of our model is that we did not include a link between lick vigor and its probability of success. As a result, when we moved the food tube away, the model did not consider the possibility that maintaining lick accuracy may involve reduced vigor. The reason for this is that we searched for but could not find a consistent relationship, across subjects or effort conditions, between protraction speed of the tongue and its success probability. Thus, we cannot exclude this alternate hypothesis. However, the most interesting aspect of our results was that when we increased tube distance, making harvest more effortful, there was not only a reduction in lick vigor, but also a reduction in saccade vigor. That is, the decisions and actions during the work period responded to the increased effort cost of reward during the harvest period.

What might be a neural basis for this coordination of decisions and movements? A clue was the fact that the pupils were more constricted in sessions in which the effort cost of harvest was greater. This global change in pupil size accompanied delayed harvest and reduced vigor across sessions, but surprisingly, even within a session, transient changes in pupil size accompanied changes in vigor. During the work period the trial-to-trial reduction in saccade vigor accompanied trial-to-trial constriction of the pupil, and within a harvest period, the rapid rise and then the gradual fall in lick vigor paralleled rapid dilatation followed by gradual constriction of the pupil.

Pupil dilation is a proxy for activity in the brainstem neuromodulatory system[33] and is a measure of arousal.[34] Control of pupil size is dependent on spiking of norepinephrine neurons in locus coeruleus (LC-NE): an increase in the activity of these neurons produces pupil dilation.[35,36] Some of these neurons show a transient change in their activity when acquisition of reward requires expenditure of either physical[11] or mental effort,[37] even when there is no concomitant movement to be made. It is possible that in the

present task, as the effort cost of harvest increased, LC-NE neurons decreased their activity, producing pupil constriction. If so, the reduced NE release may have had two simultaneous effects: encourage work and promote delayed gratification in brain regions that control decisions, discourage energy expenditure and promote sloth in brain regions that control movements. Thus, the idea that emerges is that the response of NE to economic variables, as inferred via changes in pupil size, might act as a bridge to coordinate the computations in the decision-making circuits with the computations in the motor-control circuits, aiming to implement a consistent control policy that improves the capture rate.

In addition to NE, the basal ganglia, and in particular the neurotransmitter dopamine, are likely the key contributors to the coordination of decisions with actions.[38,39] When the effort price of a preferred food increases, animals choose to work longer, pressing a lever a greater number of times.[40,41] This desire to expend effort to acquire a valuable reward is reduced if dopamine is blocked in the ventral striatum.[42–44] Hunger activates circuits in the hypothalamic nuclei, disinhibiting dopamine release in response to food cues.[45] Dopamine concentrations in the striatum drop when the effort price of a food reward increases,[46] and dopamine release before onset of a movement tends to invigorate that movement.[47] Thus, the presence of dopamine may not only alter decisions by encouraging expenditure of effort, but also modify movements by promoting vigor.

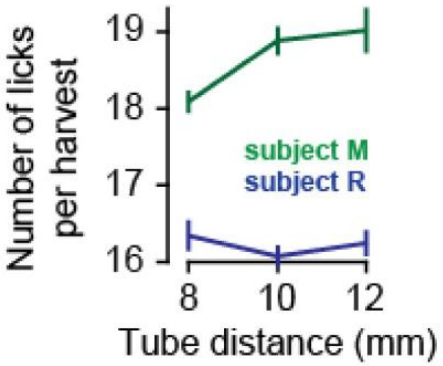
Experiments of Hayden et al.[48] and Barack et al.[49] suggest that the decision of when to stop work and commence harvest may rely on computations that are carried out in the cingulate cortex. They found that as monkeys deliberated between the choice of staying and acquiring diminishing rewards, or leaving and incurring a travel cost, these neurons encoded a decision-variable that reflected the value of leaving the patch. The prediction that emerges from our work is that the rate of rise of these decision variables may be modulated by the presence of NE.

From a motor control perspective, a surprising aspect of our results was that an increase in saccade vigor accompanied an improvement in endpoint accuracy. In our earlier work we found that during reaching, reward increased vigor without reducing accuracy.[50] Thus, the brain has the means to increase movement vigor and improve its accuracy. How is this achieved?

We found that the high vigor saccades were produced when the pupils were dilated, implying an increased release of NE. In songbirds, increased NE release acts on the basal ganglia to suppress activity of spiny neurons, and this reduced activity in the basal ganglia accompanies reduced variance in the songs that the animal sings.[51] Thus, NE may play a critical role in control of movement variability. For saccades, control of endpoint accuracy depends on the coordinated activity of Purkinje cells in the oculomotor region of the cerebellar vermis.[12,52] LC projects to the cerebellum, and stimulation of LC neurons increases the sensitivity of Purkinje cells to their inputs.[53]

Is movement vigor increased following increased NE inputs from LC to the basal ganglia, and accuracy improved following increased NE inputs from LC to the cerebellum? Does decision-making shift toward greater work and delayed gratification following reduced NE inputs from LC to the frontal lobe? These are some of the questions that await future experiments.

Chapter 2.5. Supplementary Figures



Supplementary Figure 2.1. *Number of licks per harvest as a function of tube distance.*

Chapter 3 Control of goal-directed tongue movements by Purkinje cells of the cerebellum

Precise control of the tongue during speech, mastication, and swallowing is lost when there is damage to the cerebellum. Yet, little is known regarding the neural computations that take place in the cerebellum during tongue movements. Here, we trained head-fixed marmosets to harvest food from tubes just large enough to accommodate their tongue. We identified the lingual regions in lobule VI of the vermis and recorded from hundreds of Purkinje cells (P-cells), each in sessions where the subject produced thousands of tongue movements. To quantify contributions of a P-cell to control of the tongue, we relied on the fact that in a small fraction of the licks, the input from the inferior olive caused a complex spike (CS), which then briefly silenced the P-cell. In nearly every P-cell, for both ipsilateral and contralateral targets, the CS rates increased during protraction, then declined during retraction, thus specifying the preferred direction of motion in the olivary input, termed CS-on. We compared the tongue's trajectory in the movement that had experienced the CS-induced SS suppression with temporally adjacent licks that had not. If the suppression occurred during protraction, the tongue exhibited hypermetria, and if the suppression took place during retraction, the tongue exhibited slowing. These effects amplified when two P-cells were simultaneously suppressed. Therefore, suppression of P-cells in the lingual vermis disrupted the forces that would normally decelerate the tongue as it approached the target, demonstrating a specialization in stopping the movement. The CS-on direction tended to align with the direction of downstream forces produced during P-cell suppression, suggesting that the olivary input defines the axis of movement that the simple spikes contribute to.

Chapter 3.1. Introduction

We use our tongue for verbal communication and mastication, skills that require the brain to control more than 100 muscles simultaneously[54]. Damage to the cerebellum disrupts both types of movements, resulting in abnormal muscle activation patterns[55] that bear a resemblance to control of the arm[56].

Indeed, removal of the cerebellum, or inactivation of the cerebellar deep nuclei, does not prevent licking (in mice), but reduces endpoint accuracy[57]. If the activities of Purkinje cells (P-cell) are disrupted via silencing of molecular layer interneurons, the tongue's trajectory becomes erratic and the subject is no longer able to efficiently harvest liquid rewards[58]. Thus, the role of the cerebellum in control of the tongue may be similar to its role in control of the limbs and the eyes: stopping movements on target. But how might the cerebellum achieve this?

In primates, stimulation of the fastigial nucleus produces tongue movements predominantly in the ventral-dorsal axis, while stimulation of the dentate nucleus produces motion mainly in the lateral-medial axis[59]. Notably, activation of tongue muscles is most readily produced via stimulation of the fastigial nucleus (as compared to the other cerebellar nuclei)[59], suggesting that a prominent role may be played for control of the tongue by the P-cells that are located in the vermis. Unfortunately, there are no previous recordings that we know of from the P-cells in the vermis, but more is known regarding activity of P-cells in Crus I and II regions (in rodents). Before start of a bout, in Crus I and II some P-cells show an increase in their simple spikes (SS), while a smaller number show a decrease[60]. Once the licking begins, the SS rates as a population are phase-locked to the rhythm of the lick, with rate maxima occurring near lick onset[57]. Complex spikes (CSs) also exhibit their highest rates during protraction[60,61]. The challenge is to understand the relationship between the activities of P-cells and their downstream effects on control of the tongue.

To approach this question, here we relied on the fact that the inferior olive not only transmits sensory events to the cerebellum[62–64], it also transmits information regarding the direction of the planned movements[12,62]. The result is a complex spike that briefly suppresses the ability of the P-cells to generate SSs[63,64], which then produces a movement[65], or alters the ongoing movement[14,66]. Although the CS events are rare, occurring in around 5% of the tongue movements, they provide a unique opportunity to ask whether the resulting SS suppression has a measurable effect on tongue movements.

We trained marmosets to make dexterous tongue movements to harvest food from small tubes that were placed at oblique angles to the mouth. The subjects performed thousands of licks and we focused on triplets {n-1, n, n+1} where lick n experienced a single CS, but the temporally adjacent licks did not. Comparison of these movements revealed that the CS-induced SS suppression was followed by hypermetria of the tongue when it occurred during protraction and slowing of the tongue's return when it occurred during retraction. Regardless of whether the target of the movement was ipsilateral or contralateral to the location of the recording, as a population the CS rates were highest during protraction, termed CS-on, and lowest during retraction, termed CS-off. Critically, the CS-on direction coincided with the direction of downstream forces that the SS suppression induced on the tongue's trajectory. Thus, the encoding of the sensorimotor space by the climbing fiber input coincided with the downstream effects that the SS suppression had on control of the tongue. Because a similar phenomenon is present among P-cells that contribute to control of the eyes[14,62], the results raise the possibility of a common architecture of control by the cerebellum across disparate types of movements.

Chapter 3.2. Methods

We collected neurophysiological data from the cerebellum of three marmosets as they performed a saccade task and then licked to harvest their reward (Callithrix Jacchus, two males and a female, 350-370 g, subjects C, R, and M, 6 years old). We used tetrodes, heptodes, and silicon probes to measure extracellular activities of neurons, and then tracked their eyes and their tongue using video.

The marmosets were born and raised in a colony that Prof. Xiaoqin Wang has maintained at the Johns Hopkins School of Medicine since 1996. The procedures on the marmosets were evaluated and approved by the Johns Hopkins University Animal Care and Use Committee in compliance with the guidelines of the United States National Institutes of Health.

Chapter 3.2.1. Data acquisition

Following recovery from head-post implantation surgery, the animals were trained to make saccades to visual targets and rewarded with a mixture of applesauce and lab diet[13] (**Figure 3.1**). Binocular eye movements were tracked at 1000 Hz using EyeLink in subject R and M, and 2000 Hz using VPIX in subject C. Tongue movements were tracked with a 522 frame per second Sony IMX287 FLIR camera, with frames captured at 100 Hz. Visual targets were presented on an LCD screen (Subject R and M: curved MSI 32" 144 Hz - model AG32CQ, Subject C: xx). Timing of target presentations on the video screen was measured using a photo diode.

We collected MRI and CT imaging data for each animal and designed an alignment system that defined trajectories from the burr hole to various locations in the cerebellar vermis, targeting points in lobule VI [13]. We used a piezoelectric, high precision microdrive (0.5 micron resolution) with an integrated absolute encoder (M3-LA-3.4-15 Linear smart stage, New Scale Technologies) to advance the electrode. We recorded from the cerebellum using quartz insulated 4 fiber (tetrode) or 7 fiber (heptode) metal core (platinum/tungsten 95/05) electrodes (Thomas Recording), and 64 channel checkerboard or linear high density silicon probes (M1 and M2 probes, Cambridge Neurotech). We connected each electrode to a 32 or 64 channel head stage amplifier and digitizer (RHD2132 and RHD2164, Intan Technologies, USA), and then connected the head stage to a communication system (RHD2000 Evaluation Board, Intan Technologies, USA). Data were sampled at 30 kHz and band-pass filtered (2.5 - 7.6 kHz). We used OpenEphys[67] for electrophysiology data acquisition, and then used P-sort[68] to identify the simple and complex spikes in the heptodes and tetrodes recordings, and Kilosort and Phi[69] to identify the spikes for the silicon probes.

Our data was composed of 217 P-cells that were identified because of the presence of CSs. Among these neurons, we also had excellent isolation of SSs in 97 P-cells. Furthermore, we identified an additional 45

putative P-cells with excellent isolation of SSs, but no presence of CSs. Included in this data were 510 pairs of simultaneously recorded P-cells.

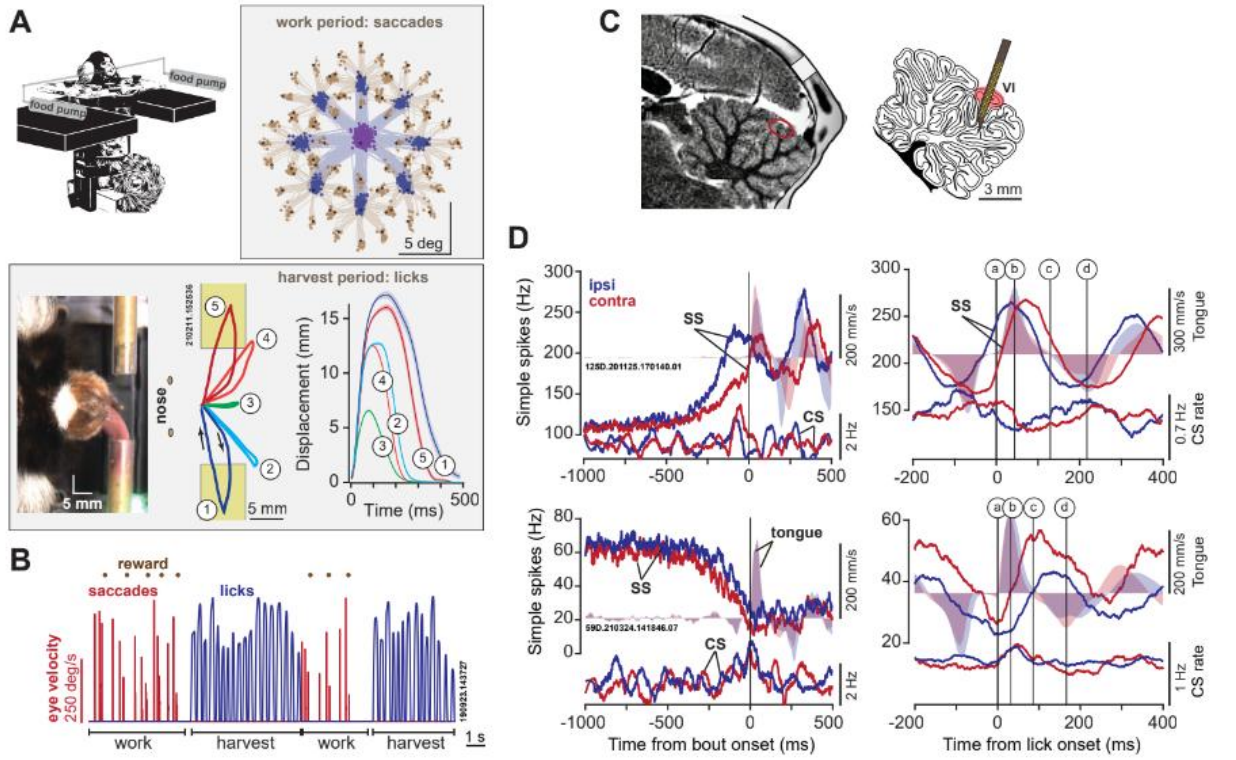


Figure 3.1. *Marmosets produced dexterous tongue movements during recordings from lobule VI of the cerebellar vermis. A. Subjects made saccades to visual targets and received a small amount of food as reward, delivered via one of two tubes places obliquely to the mouth. In task relevant movements, they directed their tongue to the edge of the tube to harvest food near the tip (2, 4), or inside the tube to harvest food that was deeper (1, 5). In task irrelevant movements, they groomed their face (3). B. Subjects chose to work for consecutive trials, allowing the food to accumulate, then harvested the food in bouts of licking. C. We employed silicon probes to record from lobule VI of the vermis. D. Simple and complex spikes (SS, CS) of two Purkinje cells, aligned to bout onset and lick onset. A single lick was divided into acceleration period of protraction (a-b), deceleration period of protraction (b-c), and acceleration period of retraction (c-d). Filled color curves indicate tongue velocity*

Chapter 3.2.2. Behavioral protocol

Each trial began with a saccade to the center target followed by fixation for 200 ms, after which a primary target (0.5x0.5 deg square) appeared at one of 8 randomly selected directions at a distance of 5-6.5 deg (**Figure 3.1**A). Onset of the primary target coincided with presentation of a tone. As the animal made a saccade to the primary target, that target was erased, and a secondary target was presented at a distance of 2-2.5 deg, also at one of 8 randomly selected directions. The subject was rewarded if following the

primary saccade, it made a corrective saccade to the secondary target, landed within 1.5 deg radius of the target center, and maintained fixation for at least 200 ms. The onset of reward coincided with presentation of a second, distinct tone. Following an additional 150-250 ms period (uniform random distribution), the secondary target was erased, and the center target was displayed, indicating the onset of the next trial. Thus, a successful trial comprised of a sequence of 3 saccades: center, primary, and corrective, after which the subject received a small increment of food (0.015 mL).

To produce goal-directed licking, the food was provided in two small tubes (4.4 mm diameter), one to the left and the other to the right of the animal (**Figure 3.1**A). A successful trial produced a food increment in one of the tubes and would continue to do so for 50-300 consecutive trials, then switch to the other tube. Because the food increment was small, the subjects naturally chose to work for a few consecutive trials, tracking the visual targets and allowing the food to accumulate, then stopped tracking and harvested the food via a licking bout. The licking bout typically consisting of 15-40 licks[70]. The subjects did not work while harvesting, and often fixated the tube. As a result, the behavior consisted of a work period of targeted saccades, followed by a harvest period of targeted licking (**Figure 3.1**B), repeated hundreds of times per session.

Chapter 3.2.3. Data analysis

We analyzed tongue movements using DeepLabCut[15]. Our network was trained on 89 video recordings of the subject with 15-25 frames extracted and labeled from each recording. The network was built on the ResNet-152 pre-trained model, and then trained over 1.03x106 iterations with a batch size of 8, using a GeForce GTX 1080Ti graphics processing unit. A Kalman filter was further applied to improve quality and smoothness of the tracking, and the output was analyzed in MATLAB to quantify varying lick events and kinematics.

We tracked the tongue tip and the edge of the food in the tube, along with control locations (nose position and tube edges) (**Figure 3.1**A). We tracked all licks, regardless of whether they were aimed toward the tube (reward seeking), or not (grooming).

Simple and complex spike baseline firing rates were computed by dividing the total number of spikes by the duration of the entire recording. Simple and complex spike instantaneous firing rate were calculated from peri-event time histograms with 1 ms bin size. We used a Savitzky–Golay filter (2nd order, 31 datapoints) to smooth the traces for visualization purposes.

Chapter 3.2.4. Computing the kinematic effects of CS-induced SS suppression

For each P-cell we considered triplets of consecutive tube-directed licks {n-1, n, n+1}, where all three licks were of the same type, i.e., contacted the same part of the tube (edge or inner). We then selected the subset of triplets in which there was a CS at only a single period in lick n, but no CS during all periods in the two neighboring licks n-1, and n+1. We then compared tongue trajectories between the lick that had a CS with the two neighboring licks, i.e., n-(n-1) and n-(n+1).

To compute the bounds for the null hypothesis, we used bootstrapping to compute 95% confidence intervals. We shuffled the assignment of CS tags from the lick in which it had occurred to a randomly assigned lick of the same type. Using this pseudo-data, we then selected triplets of consecutive tube-directed licks and computed trajectory differences among neighboring licks, averaging n-(n-1) and n-(n+1). We computed this expected value for each cell, computed a mean across all the cells, and then repeated the shuffling 30 times to compute 95% confidence intervals.

Chapter 3.3. Results

We tracked the eyes and the tongue of head-fixed marmosets (n=3, subjects M, R, and C) as they performed visually guided saccades in exchange for food (**Figure 3.1**A). The subjects performed a sequence of 3 visually guided saccades for a successful trial, at the end of which we delivered an increment

of food (slurry mixture of apple sauce and monkey chow). This food was provided via either the left or the right tube for 50-300 consecutive trials, and then switched tubes. Because the amounts were small (0.015-0.02 mL), and the tubes were located at ±90° with respect to the mouth, harvesting was effortful[73], requiring skillful movements toward a target that was just large enough to accommodate the tongue (4.4 mm diameter tube). As a result, the subjects naturally chose to work for a few consecutive trials, allowing the food to accumulate, then stopped working and harvested through a bout of licking (**Figure 3.1**B).

The tongue movements were of two general types, tube directed or grooming (**Figure 3.1**A). In tube directed licks, the tongue either glanced the edge of the tube to harvest the food that was near the tip (**Figure 3.1**A, labeled 2&4), or penetrated the tube to harvest the food that was deeper (**Figure 3.1**A, labeled 1&5). During a typical 2-3 hour recording session, the subjects performed n=3909.08+/-9.77 targeted licks (i.e., aimed at a tube), and n=1173.64+/-3.82 grooming licks (**Supplementary Figure 3.1**). We began with focusing on the targeted tongue movements.

We tracked the motion of the tongue using DeepLabCut[15], and combined MRI and CT image guided procedures[13] to place heptodes and silicon probes in lobules VI and VII of the vermis. Over the course of 2.5 years, we recorded from n=262 P-cells (**Figure 3.1**C). A neuron was identified as a definitive P-cell (n=217) because of the presence of complex spikes (CS). In addition, we included data from putative P-cells (n=45) for which we could not isolate the CSs but the neuron was located in the P-cell layer and exhibited 0 ms synchronous simple spike (SS) interactions with other confirmed P-cells[12,62] (Supplementary Fig. 2).

We classified tongue motion based on whether it was targeting the ipsilateral tube or the contralateral tube with respect to the site of the recording. For example, **Figure 3.1**D illustrates the activities of two P-cells. One P-cell increased its SS activity ~250 ms before bout onset, earlier for the ipsilateral target, while another P-cell decreased its SS activity, also ~250 ms before bout onset but earlier for the contralateral target. As the bout began, the CS rates appeared to increase briefly in both P-cells

while the SS rates were modulated in a rhythmic pattern that appeared related to the various periods of the lick. We labeled these periods as protraction acceleration (**Figure 3.1**D, a-b), protraction deceleration (b-c), and retraction acceleration (c-d). Our aim was to ask whether the spikes that were generated by each P-cell had a causal downstream effect on the motion of the tongue, and if so, what was this contribution.

Chapter 3.3.1. CS-induced SS suppression produced overshooting of the tongue during protraction, and slowed return during retraction

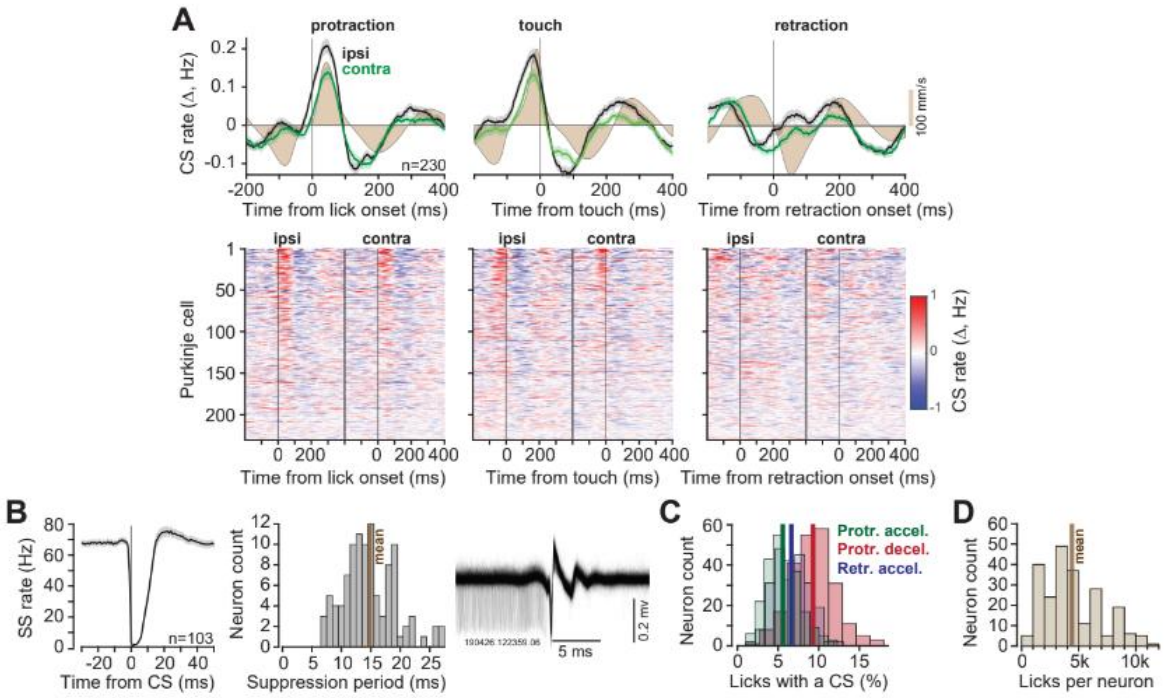


Figure 3.2. *CS rates increased with protrusion and decreased with retraction.*
A. CS rates across the population aligned to protraction onset, touch of the tube, and retraction onset. B. CS induced SS suppression, averaged across the subset of P-cells for which both the CS and the SS were isolated (left, n=97). Example of SS and CS waveforms for a single P-cell are shown at right. C. CS activity across all P-cells, aligned to protraction, touch, and retraction, sorted based on CS rate for contralateral licks at lick onset. D. Percentage of licks with a CS during a specific period of time for each neuron. E. Number of task relevant licks per neuron. Error bars are SEM.

As a population, the n=217 confirmed P-cells exhibited CS rates that increased near the onset of protraction (**Figure 3.2**A and **Figure 3.2**C), peaking around the time the tongue touched the tube, and then

decreased below baseline at retraction onset. These rate changes were slightly greater for ipsilateral licks (0.05+/-0.03 Hz, within cell difference, mean+/-SEM).

As expected, each CS suppressed the P-cell's SS production (**Figure 3.2**B, left: all P-cells, right: single P-cell) such that during licking, the suppression lasted an average of 14.5±0.45 ms (time to 80% recovery of SS rate, mean±SEM). However, CS events were rare. A CS occurred in only 5.35±0.01% of the licks during protraction acceleration period (mean±SEM), 8.60±0.01% of the licks during protraction deceleration period, and 6.63±0.009% of the licks during retraction acceleration period (**Figure 3.2**D). Because our intention was to ask whether the CS-induced SS suppression had downstream effects on the motion of the tongue, to counter the low CS probability we strived to maintain good cell isolation so that we could collect a larger number of trials for each neuron. For a typical P-cell we acquired a dataset of 5082.72+/-13.03 licks (**Figure 3.2**E).

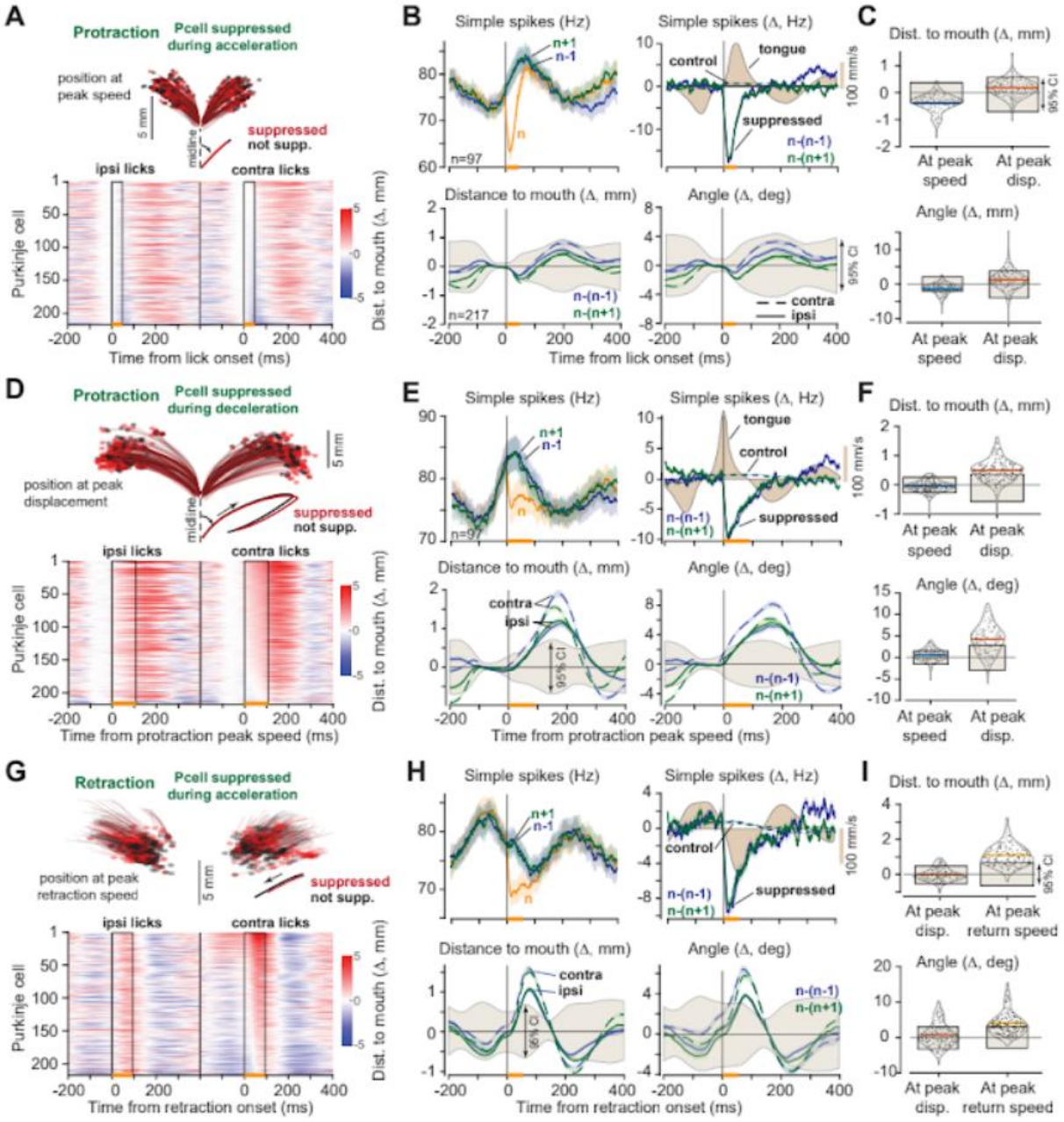


Figure 3.3. *CS-induced SS suppression produced hypermetria during protraction and slowing during retraction.*
A. Suppression during the acceleration period of protraction (orange bar). Traces show average tongue trajectory for each P-cell during suppressed and control licks. Ipsilateral licks are shown to the left and contralateral to the right. Heatmap quantifies change in endpoint trajectory between suppressed and control licks for each cell. B. Top row: SS rates for licks {n-1, n, n+1}, where only lick n experienced a CS. Filled color curves indicate tongue velocity. Second row: trajectory of the tongue in lick n as compared to its two temporally neighboring licks. Trajectory is measured via distance from tip of the tongue to the mouth and angle of the tip with respect to midline. The filled region is 95% CI. C. Distance to mouth and angle in lick n as compared to neighboring licks. Shaded region is 95% CI. D-F. Suppression during the deceleration period of protraction induces hypermetria. Same format as in part A-C. G-I. Suppression during the acceleration period of retraction induces slowing. Same format as in part A-C. Error bars are SEM.]

For each P-cell we considered triplets of consecutive licks $\{n-1, n, n+1\}$, where all three licks were of the same type, i.e., contacted the same part of the tube (edge or inner). We then selected the subset of triplets in which there was a CS at only a single period in lick n, but no CS during all periods in the two neighboring licks $n-1$, and $n+1$. For example, consider tongue trajectories in which there was a CS during the acceleration period of protrusion (**Figure 3.3**A). This period was brief (47.86±0.02 ms in duration), during which the SS activity was normally rising and nearly identical in licks $n-1$ and $n+1$ (**Figure 3.3**B, 1st row), but suppressed during lick n. We measured the change in SS activity by comparing lick n with licks $n-1$ and $n+1$ and plotted the results of each comparison in **Figure 3.3**B, green & blue solid lines (labeled suppressed, top row, right column). As a control, we performed a bootstrapping procedure in which we generated a pseudo data set for each P-cell by randomly assigning the CS label to a lick and comparing it with its two neighbors. As expected, in trials in which there was a CS, the SSs were suppressed during the acceleration period of protraction, but then rapidly recovered.

To ask whether there were any effects of this brief SS suppression on tongue kinematics, we measured the distance of the tongue tip to the mouth, and also its angle with respect to the midline, and then compared the SS suppressed trajectories with the neighboring licks (in which a CS was absent). The effects appeared consistent among the P-cells: following SS suppression, the tongue was displaced outwards (**Figure 3.3**A, red colors). However, statistical testing, which relied on bootstrapping procedure to compute 95% confidence intervals (CI), demonstrated that the changes were within the error bounds. That is, suppression of P-cells during the acceleration period of protraction had no significant effects on tongue motion (**Figure 3.3**C, measured via distance to the mouth, and its angle, at peak protraction speed and peak displacement).

However, as the protraction proceeded, the effects of SS suppression became larger. During the deceleration period of protraction, the suppression was followed by significant extension of the tongue (**Figure 3.3**E, second row), resulting in increased displacement and increased angle of the tongue's

trajectory (**Figure 3.3**F, 4.26+/-0.01 [-2.99 2.82] deg, 0.49+/-0.002 [-0.59 0.35] mm, mean+/-SEM [95% CI]). These effects were present in both ipsilateral and contralateral licks, consistent across the P-cells (**Figure 3.3**D, red colors), but larger for the contralateral licks. Notably, the effects were similar regardless of whether lick n was compared to the previous lick ($n-1$), or the subsequent lick ($n+1$) (**Figure 3.3**E, second row, blue and green).

The results hinted that the effects of SS suppression were to produce downstream forces that pushed the tongue outwards, preventing normal deceleration, resulting in over-extension. If this interpretation was valid, then the same suppression during the retraction period might produce forces that were again in the extension direction, which would impede the tongue's return. That is, if SS suppression during protraction sped the movement outward, then the same suppression during retraction should slow the movement.

To test this prediction, we considered the acceleration period of retraction. As retraction began, both the population CS activity (**Figure 3.2**A), and the population SS activity had transitioned to below baseline (**Figure 3.3**H, left). Remarkably, the CS-induced SS suppression again displaced the tongue outwards: comparison of lick n with $n-1$ or $n+1$ revealed a consistent effect: an increased distance and angle of the tongue to the mouth (**Figure 3.3**I, 3.97+/-0.02 [-3.09 3.17] deg, 1.09+/-0.003 [-0.64 0.66] mm, mean+/-SEM [95% CI]). These effects were present for ipsilateral and contralateral licks, larger for the contralateral licks, and consistent across the P-cells (**Figure 3.3**G, red colors). Thus, SS suppression during retraction slowed the return of the tongue.

The fact that a CS was present during a given period of lick n may have been because earlier in the tongue's trajectory there was an event (for example, an error), that affected that movement, increasing the likelihood of a CS, and possibly resulting in compensatory movements that followed the CS. As a control, for each period during which we had found a CS we considered the tongue's trajectory in the same lick but during the period preceding the CS. For example, for the licks in which there was a CS in

the protraction deceleration period we focused on the preceding acceleration period. In comparing the lick in which the CS had occurred with its two neighbors, we found that the distance to mouth and angle of the tongue at peak speed was not different than chance (**Figure 3.3**F, 0.61+/-0.006 [-1.59 3.17] deg, -0.05+/-0.001 [-0.27 0.26] mm, mean+/-SEM [95% CI]). We found similar results when we considered licks in which there was a CS in the retraction period: at peak protrusion the distance to mouth and tongue angle were not different than chance (**Figure 3.3**I, 0.71+/-0.02 [-3.38 3.22] deg, -0.01+/-0.002 [-0.51 0.49] mm, mean+/-SEM [95% CI]), yet the return was slowed (**Figure 3.3**I). Thus, the tongue trajectory before the CS was not different than neighboring licks yet differed after the CS-induced SS suppression.

In summary, when a CS-induced SS suppression occurred during the deceleration period of the tongue's protrusion, the tongue overextended (as compared to when the SS was not suppressed). When this suppression occurred during retraction, the tongue's return was slowed. These effects were present for targets on both the ipsilateral and contralateral sides, but greater when the target was contralateral to the site of recording. Thus, it appeared that the downstream effects of SS suppression were to add forces toward extension, or equivalently, reduce forces that would assist stopping or retracting the tongue.

Chapter 3.3.2. Perturbations scaled when pairs of P-cells were simultaneously suppressed

In a subset of recordings, we were able to simultaneously isolate 2 or more P-cells. This provided the opportunity to test whether near simultaneous CS-induced suppression of 2 P-cells had a greater effect on tongue kinematics as compared to when only one of the two P-cells was suppressed.

Our dataset included n=510 pairs of P-cells. As before, we collected triplets of consecutive licks $\{n-1, n, n+1\}$ where all the licks were of the same type (directed toward the same part of the tube), but only lick n had a CS. We divided the triplets based on whether a CS was present in only one of the P-

cells, or both P-cells, then computed trajectory differences between licks n and $n-1$, and licks n and $n+1$. Finally, for each pair of P-cells we averaged $n-(n-1)$ and $n-(n+1)$ to increase statistical power (because there were far fewer licks in which both P-cells experienced a CS).

We found that if the CS occurred in both P-cells during the deceleration phase of protraction, then there was significantly greater displacement of the tongue, and its angle, as compared to when only one of the P-cells was suppressed (**Figure 3.4**A). Similarly, when the suppression occurred during retraction, the return phase of the movement experienced a greater slowing in the case of 2 P-cells as compared to a single P-cell (**Figure 3.4**B). Thus, a near simultaneous suppression of 2 P-cells amplified the kinematic effects on tongue trajectory.

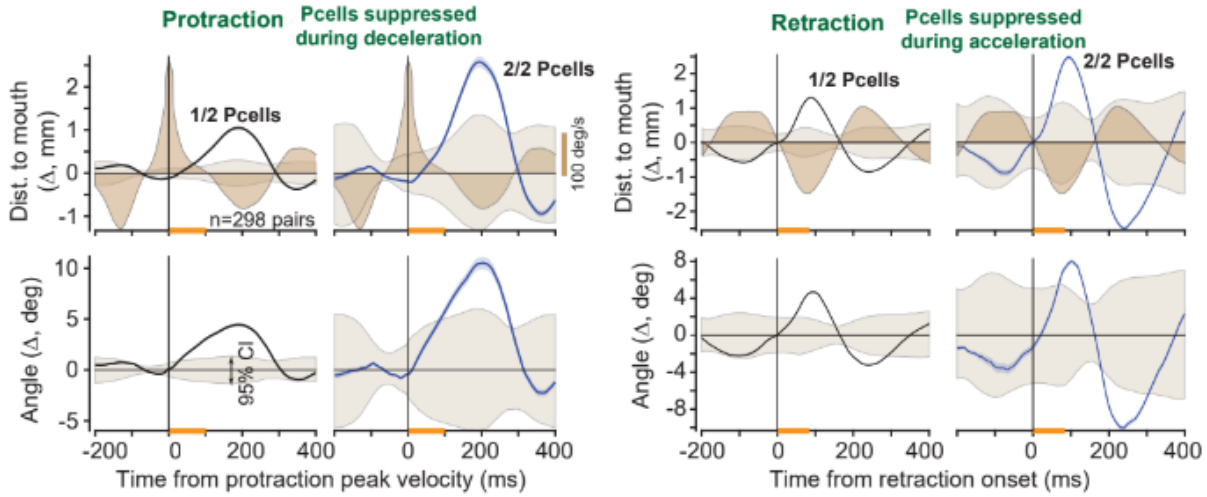


Figure 3.4. *Suppression of multiple P-cells scaled the perturbation to the tongue.*
A. Kinematic effects of CS-induced P-cell suppression during the deceleration period of protraction (orange bar). Traces show change in tongue trajectory in suppressed licks vs. control licks, measured via distance from tip of the tongue to the mouth and angle of the tip with respect to midline. Gray shaded region is 95% CI. Brown filled region is tongue velocity. B. Kinematic effects of P-cell suppression during the acceleration period of retraction (orange bar). Same format as in part A. Error bars are SEM.

Chapter 3.3.3. The effects of SS suppression were consistent across P-cells regardless of their SS modulation

A surprising result was that across nearly every P-cell, the CS-induced SS suppression was followed by an extension of the tongue (**Figure 3.3**D, G). Yet, before the bout onset, some P-cells had increased their SS

rates, while others had decreased (**Figure 3.1**D). Did the kinematic effects of SS suppression differ in these two groups?

In our data set (n=142) most P-cells (n=120) increased their SS rates before the onset of the bout, but a minority exhibited a decrease (n=22) (**Figure 3.5**A-B). We separated the P-cells into SS increasers and decreasers and found that unlike the SS rates, the CS rates increased in both groups near bout onset (**Figure 3.5**C). We then compared tongue trajectories in triplets of consecutive licks $\{n-1, n, n+1\}$, finding that during protraction, following the CS-induced SS suppression in the deceleration period, in both groups of P-cells the tongue trajectory was displaced away from the mouth, exhibiting a greater distance and angle (**Figure 3.5**D). Similarly, during retraction, SS suppression in both groups of P-cells produced a slowing of the tongue's return, resulting in a greater distance and angle (**Figure 3.5**E).

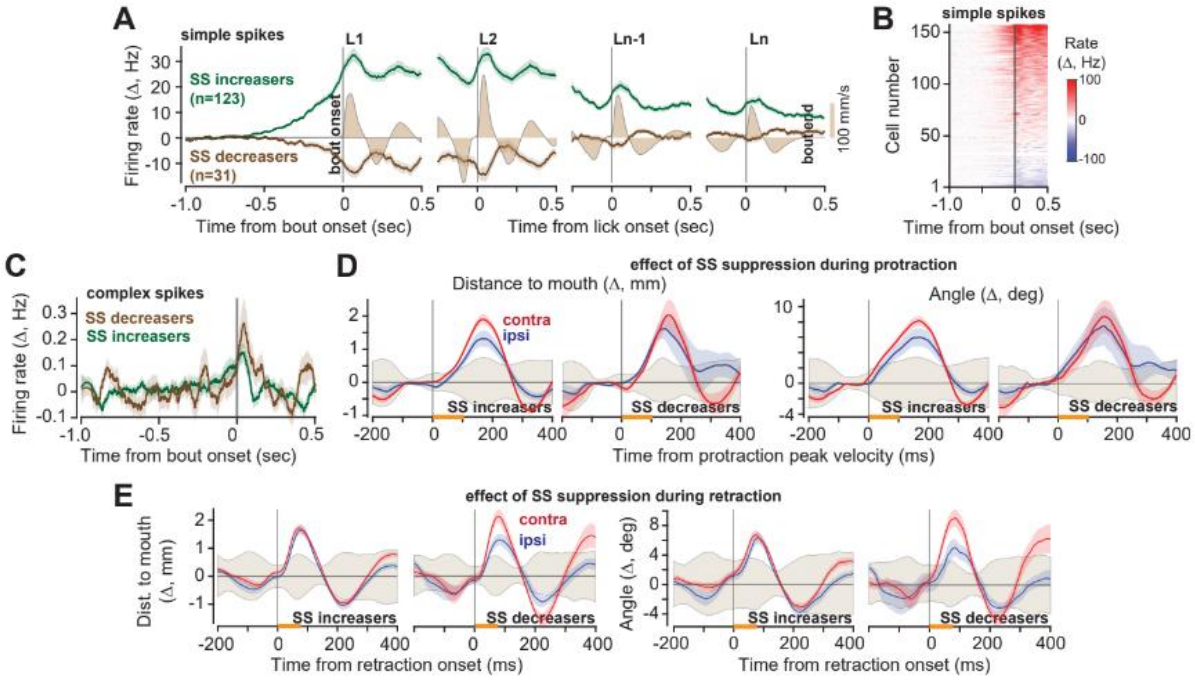


***Figure 3.5**. Effects of suppression remained consistent across P-cells regardless of SS modulation.*
A. Some of the P-cells exhibited an increase in SS rates before bout onset, while others exhibited a decrease. L1 is first lick in the bout, Ln is last lick. B. Change in SS rates for all P-cells (with respect to baseline), aligned to bout onset. C. Change in complex spike rate for the same P-cells. D. Kinematic effects of SS suppression during the deceleration period of protraction (orange bar). Shaded region is 95% CI. E. Kinematic effects of SS suppression during the acceleration period of retraction (orange bar). Error bars are SEM.

Chapter 3.3.4 The population SS response encoded the parameters of tongue kinematics

In order to organize the P-cells into a population, we relied on the fact that the downstream effects of SS suppression, for both increasers and decreasers, in both ipsilateral and contralateral directions, were to produce forces that extended the tongue. Thus, we combined all cells and computed a population response during various phases of tongue movements.

Across the cells, the CS rates peak at approximately the timepoint of maximum protraction velocity (**Figure 3.6**A&B), exhibiting a greater rate for movements toward the ipsilateral side. In contrast, the CS rates declined below baseline before the onset of retraction (**Figure 3.6**C). Thus, the CS-on direction across the P-cells was protraction, whereas CS-off was retraction, suggesting that the CS-on direction aligned with the downstream effects of SS suppression. This correspondence between the vector that describes the direction of CS-on, and the vector that describes the effects of SS suppression, is notable because the same principle holds for P-cells in the oculomotor region of the cerebellum during saccadic eye movements[14].

If a reduction in SS rates produced downstream forces that pulled the tongue outwards toward the target, then during deceleration the SS rates should increase, thus commanding forces that would stop the motion of the tongue. To analyze the SS activities as a population, we had to consider the fact that during a bout, as the SS rates modulated about a mean, the mean was not stationary [73](**Figure 3.5**A). Rather, the mean SS rates rose or fell at bout onset, then drifted back toward the values before start of the bout, reaching pre-bout levels at bout ended. Thus, to quantify modulation of SS rates, for each P-cell we considered a 2 sec moving window to compute the running average of its firing rate, then computed the SS rates with respect to this mean. The 2 sec window was chosen because it was roughly an order of magnitude larger than the duration of a typical lick.

We found that the SS rates peaked near protraction peak speed and were larger for contralateral licks (**Figure 3.6**B). The rates began declining at retraction onset and reached a trough near retraction peak speed (**Figure 3.6**B). To test if this modulation varied with tongue kinematics, we quantified lick vigor, defined as the peak speed of a given protraction with respect to the speed expected for a protraction of the same amplitude[19,70]. High vigor licks exhibited greater SS rates at peak protraction speed (**Figure 3.6**D). Given that SS suppression during protraction led to increased extension, if we interpret the increase in SS rates as commanding downstream forces in the opposite direction, then the increased SS rates during high vigor licks is consistent with the idea that the P-cells are firing to stop the protrusion. If true, then protractions that have the same peak speed, but a longer deceleration should not only exhibit greater SS rates at peak speed, but also a longer duration of activity above baseline. Indeed, we found that licks that had similar peek speed but longer decelerations tended to also have a longer period of SS rate increase (**Figure 3.6**E).

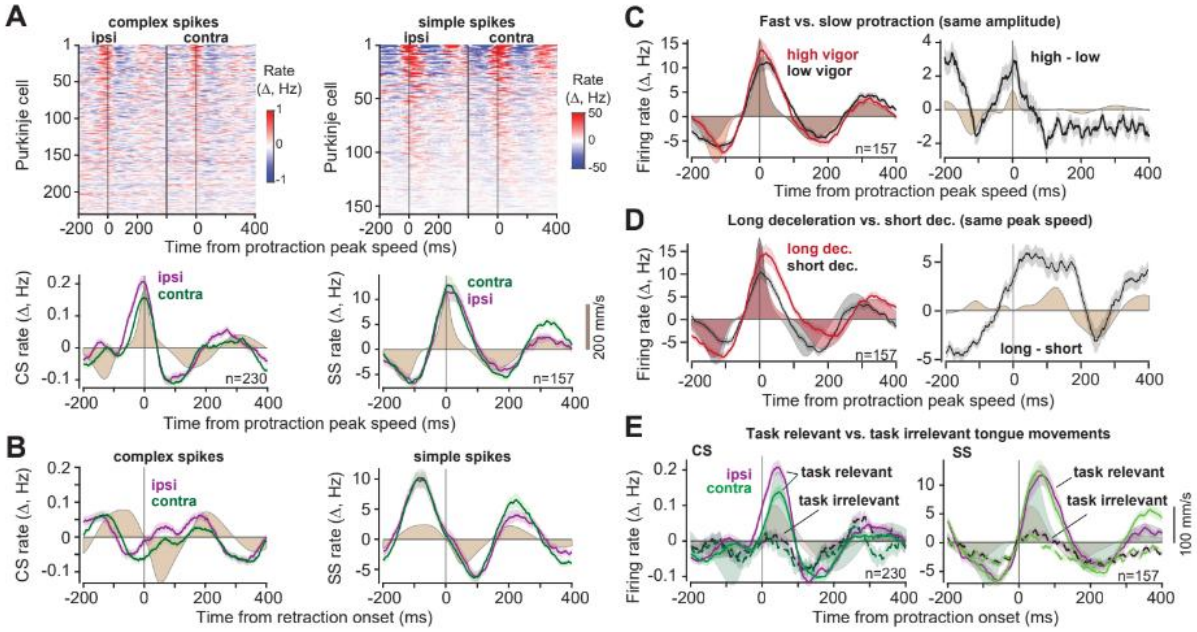


Figure 3.6. *SS rates were greater for high vigor and long deceleration licks. However, little modulation was present during task irrelevant tongue movements.*
A. CS rates across the population aligned to protraction peek speed. As a population, the direction of CS-on was protraction. B. SS rates aligned to protraction peak speed. C. CS and SS rates aligned to retraction onset. D. Left figure shows SS rates for high and low vigor protractions (same amplitude). Right figure shows within cell difference in SS rates for high minus low vigor licks. Shaded regions are tongue speed for high and low vigor licks (left) and change in speed (right). E. Left figure shows SS rates for protractions that had the same peak speed but long or short deceleration periods. Right figure shows within cell differences. Shaded regions are tongue speed for long and short deceleration period licks (left) and change in speed (right). F. Modulation of CS and SS rates during task relevant and task irrelevant licks. Light shaded region is tongue speed for task relevant movements, while dark shaded region is tongue speed for task irrelevant movements. Error bars are SEM.

Chapter 3.3.5. Control studies

The fact that a CS was present during a given period of lick n may have been because earlier in the tongue's trajectory there was an event (for example, an error), that affected that movement, increasing the likelihood of a CS, and resulting in compensatory movements that followed the CS. To check for this, for each period during which we observed a CS we considered the tongue's trajectory in the same lick but during the period preceding the CS. For example, for the licks in which there was a CS in the protraction deceleration period we focused on the protraction acceleration period. In comparing the lick in which the CS had occurred with its two neighbors, we found that in the period before the CS had occurred tongue kinematics were similar: distance to mouth and angle of the tongue at peak speed were not different than chance (**Figure 3.3**F). We made a similar observation when we considered licks

in which there was a CS in the retraction period: before the CS had occurred, at peak protrusion the distance to mouth and tongue angle were not different than chance (**Figure 3.3**l), yet the return was slowed (**Figure 3.3**). Thus, the tongue's trajectory before the CS was not different than the neighboring licks, but after the CS-induced SS suppression the trajectories diverged.

As a further control, we considered movements in which there was a CS event just before protrusion onset (**Supplementary Figure 3.4**). In these movements, the SS rates were suppressed but recovered around 10 ms after lick onset (**Supplementary Figure 3.4**, 1st row). As a result, the SS rates during the lick were indistinguishable from licks that had not been preceded by a CS. We found that in these movements, trajectory of the tongue as measured via distance and angle was not different than chance (**Supplementary Figure 3.4**, 3rd and 4th rows).

Chapter 3.4. Discussion

How does the cerebellum contribute to control of tongue movements? Here, we found that when an olivary input arrived at a P-cell, the resulting brief period of suppression prevented the normal deceleration of the tongue as it approached the target, resulting in hypermetria. When the same suppression occurred during retraction, the tongue's return was slowed. These results were consistent for both ipsilateral and contralateral targets. Notably, if the suppression was present in pairs of simultaneously recorded P-cells, the effects were magnified. Thus, regardless of whether the suppression occurred during protraction or retraction, the downstream effects were forces that pulled the tongue outwards. Because during unperturbed movements the SS rates reached their maximum at peak velocity of protraction, we infer that the consequence of this activity is to decelerate the tongue. This implies that the contributions of the cerebellum to control of tongue movements is similar to that of the eyes [71,72] and the limbs [73]: stopping the movement on target.

Like the SS rates, the CS rates peaked near protraction peak velocity, then fell below baseline before the onset of retraction. Thus, the "CS-on action" across the P-cells was protrusion, while the "CS-off action" was retraction. Notably, the downstream effects of SS suppression were to extend the tongue. Thus, there was a correspondence between the vector that described the CS-on action, and the vector that described the effects of SS suppression. This fact is notable because the same principle holds for P-cells in the oculomotor region of the cerebellum during saccadic eye movements [74]: the olivary input to an oculomotor P-cell is most active when a saccade is planned in a specific direction, and the downstream effects of that P-cell's SS suppression is to pull the eyes in the same direction. Thus, for both eye movements and tongue movements, the olivary input appears to dictate a coordinate system with which to decode the downstream contributions of a P-cell to control of that movement [75,76].

Notably, not all tongue movements engaged the cerebellum. Rather, when the purpose of the movement was to groom the face, the CS and SS rates remained near baseline during the protraction phase. This suggests that only movements that required precision engaged the P-cells.

The possible origin of climbing fiber activity at protrusion onset

We were surprised to find that the CS rates peaked not after the tongue contacted the tube, but around the time that the protraction began. This observation reproduced findings of Welsh et al. [77] in rats, who recorded from the lateral cerebellum and found that the CS rates peaked near the onset of tongue protrusion, even when the tongue was deafferented. Indeed, in all types of movements studied thus far, the CS rates appear to peak near movement onset, including walking [78], reaching [79–83], and moving the wrist [84]. For example, in the oculomotor vermis, the olivary input reports the direction of the upcoming movement near saccade onset [85]. How might the inferior olive be involved in transmitting movement information to the cerebellum?

A key observation is that the inferior olive not only receives input from the superior colliculus [86–88], but that subthreshold stimulation of a region of the colliculus leads to CS production without producing a movement [89]. Thus, it is possible that during tongue movements, the increased CS rates around the onset of protraction reflect activities of collicular, or possibly motor cortical neurons, that initiated that movement. This prediction remains to be tested with simultaneous recordings from the colliculus, motor cortex, and the cerebellum.

Preparing to initiate a tongue movement coincided with ramping activity in the P-cells

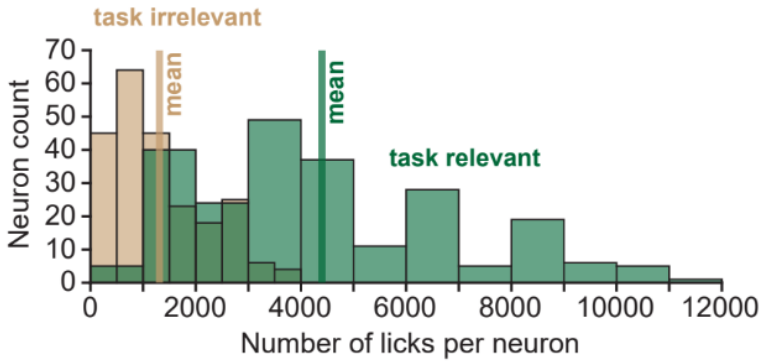
As the subject prepared to initiate a licking bout, the P-cells exhibited a ramping activity. Previous reports have noted that during this period there is ramping activity in the tongue regions of the motor cortex [90], as well as in the fastigial [90] and the dentate nuclei [91]. Inhibiting the fastigial during the ramping period disrupts planning of the movement and removes the selectivity that the motor cortical cells exhibit for direction of tongue movements [90], while inhibiting the dentate disrupts the ramping activity in the motor cortex [91]. Similarly, exciting the P-cells in the vermis abolishes the ramping activity in motor cortex during the delay period of a decision-making task [92]. This implies that as one prepares to initiate a movement, the rising activity in the motor cortex is controlled via a loop through the cerebellum. Because most of the P-cells in the vermis exhibited increasing activity during the delay period, we speculate that their role was to reduce the rate of rise in the motor cortex, effectively delaying the onset of the bout.

Using CS-induced SS suppression to infer how the P-cells contribute to control of movements

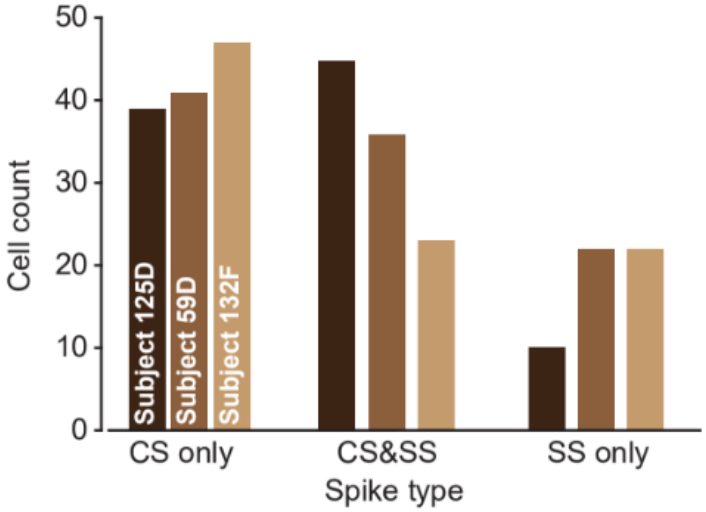
Complex spikes have baseline rates of around 1 Hz and are present in only a small fraction of the movements. For example, they are present in less than 10% of the movements as the tongue approaches the target. However, change with respect to this baseline provides information to the cerebellum regarding preceding events such as sensory prediction errors [85,93]. Thus, it was critical to test that the kinematic effects that we measured following a CS-induced SS suppression were not a consequence of a

feedback response to kinematic deviations that occurred before the CS. We did this by comparing triplets of temporally adjacent licks, finding that while the kinematics preceding the CS event remained within the chance error bounds, the kinematics that following the CS were robustly different than chance. Critically, the downstream effects of the CS-induced suppression were in the same direction, i.e., extension of the tongue, regardless of whether the event occurred during protraction or retraction.

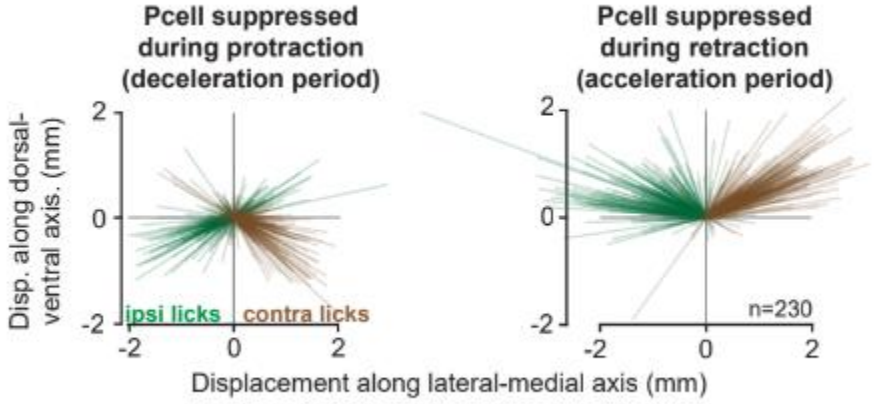
Chapter 3.5 Supplementary Figures



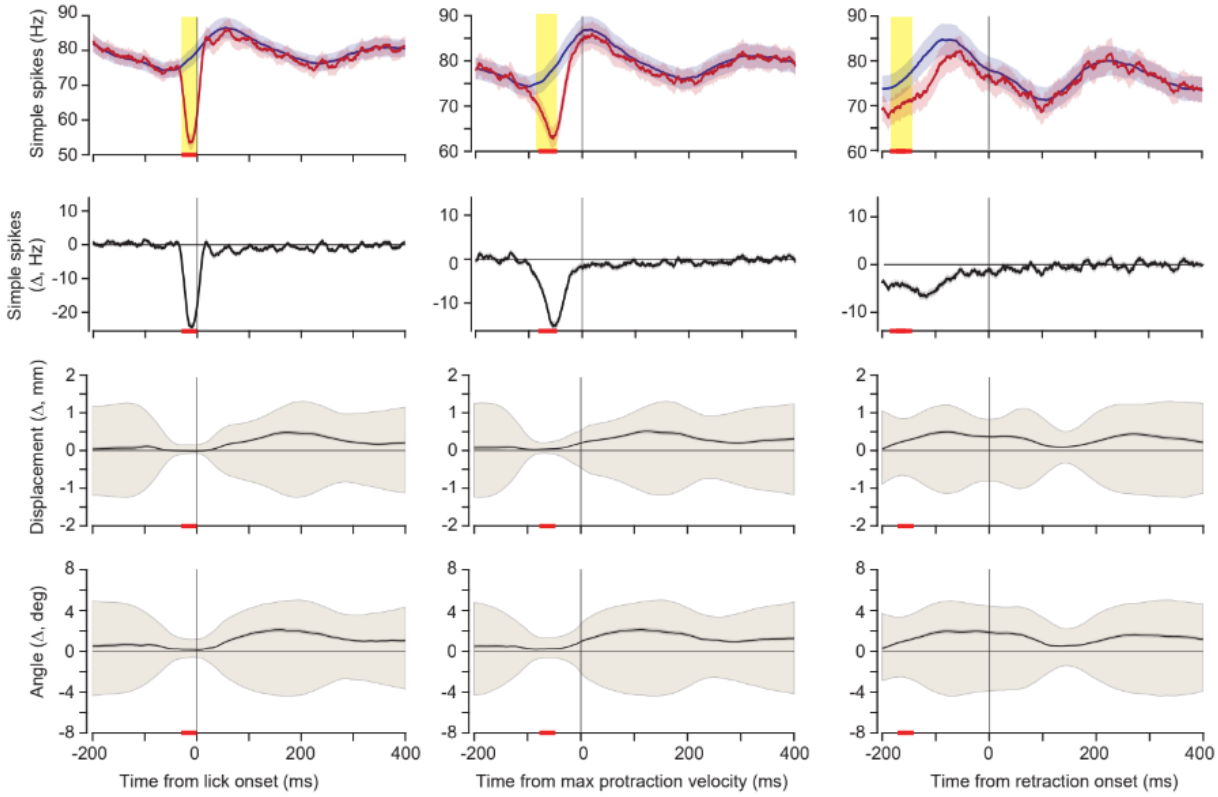
Supplementary Figure 3.1. *The number of task relevant (tube directed) and task irrelevant (grooming) licks recorded per neuron.*



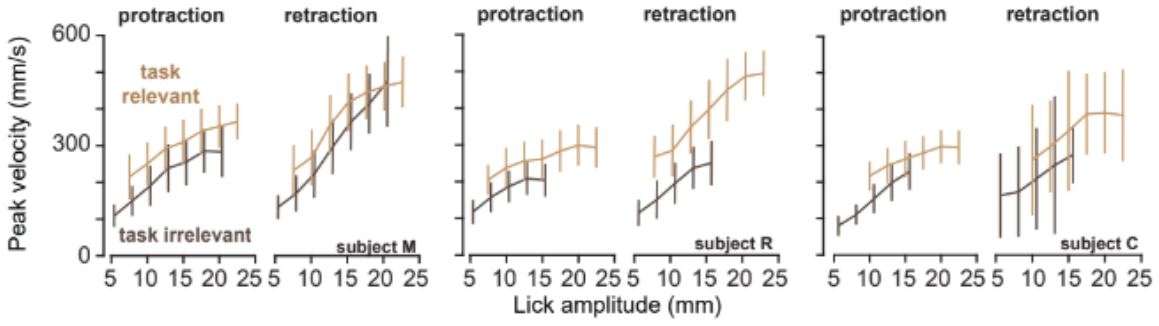
Supplementary Figure 3.2. *The number of neurons recorded from each marmoset. CS only refers to P-cells for which only the complex spikes were recorded. CS&SS refers to P-cells for which both the CS and SS were recorded. SS only refers to putative P-cells for which only the SS were recorded.*



Supplementary Figure 3.3. *Kinematic effects of CS-induced P-cell suppression in Cartesian coordinates. Left plot shows the change in the position of the tip of the tongue at the end of protraction in movements that experienced a CS during the deceleration period of protraction, with respect to movements that did not experience a CS during any period. Right plot shows the change in position of the tip of the tongue as measured at peak retraction velocity, comparing movements that experienced a CS during the retraction acceleration period with movements that did not experience a CS in any period. Each line is the average effect for a single P-cell. P-cell suppression during protraction produced hypermetria, whereas the suppression during retraction resulted in slowing.*



Supplementary Figure 3.4. *There was little or no change in lick kinematics when the CS-induced SS suppression occurred before lick onset. We chose the period following completion of one lick and the start of the next lick, which was on average 30ms in duration, i.e., the period in which the tongue was in the mouth. Top row: SS rates, aligned to lick onset, protraction peak speed, and retraction onset. Second row: change in SS rates. Third row: change in tongue displacement. Fourth row: change in tongue angle. The filled region is 95% confidence interval. Error bars are SEM.*



Supplementary Figure 3.5. *Peak velocity as a function of lick amplitude during protraction and retraction for task relevant and task irrelevant licks in each subject. Error bars are SEM.*

Chapter 4 Conclusions

Control of the tongue is crucial in a wide range of behaviors central to human experience, and its dysfunction can profoundly affect quality of life. It presents a fascinating model for studying the neural basis of fine motor control; yet there is no established primate model for the study of lingual movements. Through the work highlighted in this dissertation, we introduce the common marmoset as a promising non-human primate model for studying complex lingual movements across two domains of neuroscience: the neuroeconomics of lingual control and the neurophysiology of lingual control by the cerebellum.

In Chapter 2, we engaged two marmosets in a foraging task in which they performed saccades for food rewards and used goal-directed licks to consume rewards. We explored how economic variables such as reward and effort influenced decisions to work or harvest, as well as the vigor of saccades and licks, while manipulating the effort cost associated with harvesting. Additionally, we utilized pupillometry as a measurable proxy of internal state to gain insights into the brain's coupling of decision-making and movement vigor. We found that when the acquisition of reward became effortful, the pupils constricted, the decisions exhibited delayed gratification, and the movements displayed reduced vigor. From this coordinated response, we concluded that decisions and actions were governed as part of a single control policy aimed at maximizing a variable relevant to fitness: the capture rate.

In Chapter 3, we utilized modern high-density recording probes to capture extracellular activity of P-cells from the lingual regions of the cerebellar vermis in three marmosets as they performed goal-directed licks. We sought to develop a mechanistic understanding of how the cerebellum contributes to control of the tongue by examining the role of P-cells in enabling endpoint accuracy of tongue movements. We found that suppression of P-cell simple spike activity resulted in endpoint hypermetria of licks, inferring that P-cells played a role in aiding with lick deceleration. Furthermore, across a population of P-cells, we found that simple spike responses exquisitely encoded the deceleration window of lick protraction, scaling

as kinematics varied. We concluded that P-cells convey critical information required to stop goal-directed licks accurately at their endpoint.

Chapter 5 Bibliography

1. Charnov, E. L. Optimal foraging, the marginal value theorem. *Theor. Popul. Biol.* **9**, 129–136 (1976).
2. Cowie, R. J. Optimal foraging in great tits (Parus major). *Nature* **268**, 137–139 (1977).
3. Shadmehr, R. & Ahmed, A. A. Précis of *Vigor: Neuroeconomics of Movement Control*. *Behav. Brain Sci.* **44**, e123 (2021).
4. Richardson, H. & Verbeek, N. A. M. Diet Selection and Optimization by Northwestern Crows Feeding on Japanese Littleneck Clams. *Ecology* **67**, 1219–1226 (1986).
5. Yoon, T., Jaleel, A., Ahmed, A. A. & Shadmehr, R. Saccade vigor and the subjective economic value of visual stimuli. *J. Neurophysiol.* **123**, 2161–2172 (2020).
6. Korbisch, C. C., Apuan, D. R., Shadmehr, R. & Ahmed, A. A. Saccade vigor reflects the rise of decision variables during deliberation. *Curr. Biol.* **32**, 5374-5381.e4 (2022).
7. Shadmehr, R., Orban De Xivry, J. J., Xu-Wilson, M. & Shih, T.-Y. Temporal Discounting of Reward and the Cost of Time in Motor Control. *J. Neurosci.* **30**, 10507–10516 (2010).
8. Shadmehr, R., Huang, H. J. & Ahmed, A. A. A Representation of Effort in Decision-Making and Motor Control. *Curr. Biol.* **26**, 1929–1934 (2016).
9. Control of movement vigor and decision making during foraging. https://www.pnas.org/doi/10.1073/pnas.1812979115 doi:10.1073/pnas.1812979115.
10. Joshi, S. & Gold, J. I. Pupil Size as a Window on Neural Substrates of Cognition. *Trends Cogn. Sci.* **24**, 466–480 (2020).
11. Bornert, P. & Bouret, S. Locus coeruleus neurons encode the subjective difficulty of triggering and executing actions. *PLOS Biol.* **19**, e3001487 (2021).
12. Sedaghat-Nejad, E., Pi, J. S., Hage, P., Fakharian, M. A. & Shadmehr, R. Synchronous spiking of cerebellar Purkinje cells during control of movements. *Proc. Natl. Acad. Sci.* **119**, e2118954119 (2022).

13. Sedaghat-Nejad, E. *et al.* Behavioral training of marmosets and electrophysiological recording from the cerebellum. *J. Neurophysiol.* **122**, 1502–1517 (2019).
14. Muller, S. Z. *et al.* Complex spikes perturb movements, revealing the sensorimotor map of Purkinje cells. 2023.04.16.537034 Preprint at https://doi.org/10.1101/2023.04.16.537034 (2023).
15. Mathis, A. *et al.* DeepLabCut: markerless pose estimation of user-defined body parts with deep learning. *Nat. Neurosci.* **21**, 1281–1289 (2018).
16. He, K., Zhang, X., Ren, S. & Sun, J. Deep Residual Learning for Image Recognition. in *2016 IEEE Conference on Computer Vision and Pattern Recognition (CVPR)* 770–778 (IEEE, Las Vegas, NV, USA, 2016). doi:10.1109/CVPR.2016.90.
17. Yoon, T., Geary, R. B., Ahmed, A. A. & Shadmehr, R. Control of movement vigor and decision making during foraging. *Proc. Natl. Acad. Sci.* **115**, E10476–E10485 (2018).
18. Reppert, T. R., Lempert, K. M., Glimcher, P. W. & Shadmehr, R. Modulation of Saccade Vigor during Value-Based Decision Making. *J. Neurosci.* **35**, 15369–15378 (2015).
19. Reppert, T. R. *et al.* Movement vigor as a traitlike attribute of individuality. *J. Neurophysiol.* **120**, 741–757 (2018).
20. Foraging Theory | Princeton University Press. https://press.princeton.edu/books/paperback/9780691084428/foraging-theory (1987).
21. Bautista, L. M., Tinbergen, J. & Kacelnik, A. To walk or to fly? How birds choose among foraging modes. *Proc. Natl. Acad. Sci.* **98**, 1089–1094 (2001).
22. Sugiwaka, H. & Okouchi, H. Reformative self-control and discounting of reward value by delay or effort. *Jpn. Psychol. Res.* **46**, 1–9 (2004).
23. Prévost, C., Pessiglione, M., Météreau, E., Cléry-Melin, M.-L. & Dreher, J.-C. Separate Valuation Subsystems for Delay and Effort Decision Costs. *J. Neurosci.* **30**, 14080–14090 (2010).

24. Klein-Flügge, M. C., Kennerley, S. W., Saraiva, A. C., Penny, W. D. & Bestmann, S. Behavioral Modeling of Human Choices Reveals Dissociable Effects of Physical Effort and Temporal Delay on Reward Devaluation. *PLOS Comput. Biol.* **11**, e1004116 (2015).
25. Huang, H. J. & Ahmed, A. A. Older adults learn less, but still reduce metabolic cost, during motor adaptation. *J. Neurophysiol.* **111**, 135–144 (2014).
26. Ralston, H. J. Energy-speed relation and optimal speed during level walking. *Int. Z. Für Angew. Physiol. Einschließlich Arbeitsphysiologie* **17**, 277–283 (1958).
27. Bastien, G. J., Willems, P. A., Schepens, B. & Heglund, N. C. Effect of load and speed on the energetic cost of human walking. *Eur. J. Appl. Physiol.* **94**, 76–83 (2005).
28. Harris, C. M. & Wolpert, D. M. Signal-dependent noise determines motor planning. *Nature* **394**, 780–784 (1998).
29. Wang, C., Xiao, Y., Burdet, E., Gordon, J. & Schweighofer, N. The duration of reaching movement is longer than predicted by minimum variance. *J. Neurophysiol.* **116**, 2342–2345 (2016).
30. Lemon, W. C. Fitness consequences of foraging behaviour in the zebra finch. *Nature* **352**, 153–155 (1991).
31. Bateson, M. & Kacelnik, A. Preferences for fixed and variable food sources: variability in amount and delay. *J. Exp. Anal. Behav.* **63**, 313–329 (1995).
32. Bateson, M. & Kacelnik, A. Rate currencies and the foraging starling: the fallacy of the averages revisited. *Behav. Ecol.* **7**, 341–352 (1996).
33. Vazey, E. M., Moorman, D. E. & Aston-Jones, G. Phasic locus coeruleus activity regulates cortical encoding of salience information. *Proc. Natl. Acad. Sci.* **115**, E9439–E9448 (2018).
34. Mathôt, S. Pupillometry: Psychology, Physiology, and Function. *J. Cogn.* **1**, 16.
35. Joshi, S., Li, Y., Kalwani, R. M. & Gold, J. I. Relationships between Pupil Diameter and Neuronal Activity in the Locus Coeruleus, Colliculi, and Cingulate Cortex. *Neuron* **89**, 221–234 (2016).

36. Breton-Provencher, V. & Sur, M. Active control of arousal by a locus coeruleus GABAergic circuit. *Nat. Neurosci.* **22**, 218–228 (2019).

37. Contadini-Wright, C., Magami, K., Mehta, N. & Chait, M. Pupil Dilation and Microsaccades Provide Complementary Insights into the Dynamics of Arousal and Instantaneous Attention during Effortful Listening. *J. Neurosci. Off. J. Soc. Neurosci.* **43**, 4856–4866 (2023).

38. Thura, D. & Cisek, P. The Basal Ganglia Do Not Select Reach Targets but Control the Urgency of Commitment. *Neuron* **95**, 1160-1170.e5 (2017).

39. Herz, D. M. *et al.* Dynamic control of decision and movement speed in the human basal ganglia. *Nat. Commun.* **13**, 7530 (2022).

40. Salamone, J. D. *et al.* Haloperidol and nucleus accumbens dopamine depletion suppress lever pressing for food but increase free food consumption in a novel food choice procedure. *Psychopharmacology (Berl.)* **104**, 515–521 (1991).

41. Salamone, J. D., Wisniecki, A., Carlson, B. B. & Correa, M. Nucleus accumbens dopamine depletions make animals highly sensitive to high fixed ratio requirements but do not impair primary food reinforcement. *Neuroscience* **105**, 863–870 (2001).

42. Koch, M., Schmid, A. & Schnitzler, H.-U. Role of nucleus accumbens dopamine D1 and D2 receptors in instrumental and Pavlovian paradigms of conditioned reward. *Psychopharmacology (Berl.)* **152**, 67–73 (2000).

43. Farrar, A. M. *et al.* Nucleus accumbens and effort-related functions: behavioral and neural markers of the interactions between adenosine A2A and dopamine D2 receptors. *Neuroscience* **166**, 1056–1067 (2010).

44. Yohn, S. E. *et al.* The role of dopamine D1 receptor transmission in effort-related choice behavior: Effects of D1 agonists. *Pharmacol. Biochem. Behav.* **135**, 217–226 (2015).

45. Cassidy, R. M. & Tong, Q. Hunger and Satiety Gauge Reward Sensitivity. *Front. Endocrinol.* **8**, 104 (2017).

46. Schelp, S. A. *et al.* A transient dopamine signal encodes subjective value and causally influences demand in an economic context. *Proc. Natl. Acad. Sci.* **114**, E11303–E11312 (2017).

47. da Silva, J. A., Tecuapetla, F., Paixão, V. & Costa, R. M. Dopamine neuron activity before action initiation gates and invigorates future movements. *Nature* **554**, 244–248 (2018).

48. Hayden, B. Y., Pearson, J. M. & Platt, M. L. Neuronal basis of sequential foraging decisions in a patchy environment. *Nat. Neurosci.* **14**, 933–939 (2011).

49. Barack, D. L., Chang, S. W. C. & Platt, M. L. Posterior Cingulate Neurons Dynamically Signal Decisions to Disengage during Foraging. *Neuron* **96**, 339-347.e5 (2017).

50. Summerside, E. M., Shadmehr, R. & Ahmed, A. A. Vigor of reaching movements: reward discounts the cost of effort. *J. Neurophysiol.* **119**, 2347–2357 (2018).

51. Singh Alvarado, J. *et al.* Neural dynamics underlying birdsong practice and performance. *Nature* **599**, 635–639 (2021).

52. Barash, S. *et al.* Saccadic Dysmetria and Adaptation after Lesions of the Cerebellar Cortex. *J. Neurosci.* **19**, 10931–10939 (1999).

53. Moises, H. C., Waterhouse, B. D. & Woodward, D. J. Locus coeruleus stimulation potentiates Purkinje cell responses to afferent input: the climbing fiber system. *Brain Res.* **222**, 43–64 (1981).

54. Levelt, W. J. M. *Speaking: From Intention to Articulation*. (The MIT Press, 1989). doi:10.7551/mitpress/6393.001.0001.

55. Gentil, M. EMG analysis of speech production of patients with Friedreich disease. *Clin. Linguist. Phon.* **4**, 107–120 (1990).

56. Vilis, T. & Hore, J. Central neural mechanisms contributing to cerebellar tremor produced by limb perturbations. *J. Neurophysiol.* **43**, 279–291 (1980).

57. Bryant, J. L., Boughter, J. D., Gong, S., LeDoux, M. S. & Heck, D. H. Cerebellar cortical output encodes temporal aspects of rhythmic licking movements and is necessary for normal licking frequency. *Eur. J. Neurosci.* **32**, 41–52 (2010).

58. Gaffield, M. A. & Christie, J. M. Movement Rate Is Encoded and Influenced by Widespread, Coherent Activity of Cerebellar Molecular Layer Interneurons. *J. Neurosci.* **37**, 4751–4765 (2017).

59. Bowman, J. P. & Aldes, L. D. Organization of the cerebellar tongue representation in the monkey. *Exp. Brain Res.* **39**, 249–259 (1980).

60. Gaffield, M. A., Sauerbrei, B. A. & Christie, J. M. Cerebellum encodes and influences the initiation, performance, and termination of discontinuous movements in mice. *eLife* **11**, e71464 (2022).

61. Welsh, J. P., Lang, E. J., Suglhara, I. & Llinás, R. Dynamic organization of motor control within the olivocerebellar system. *Nature* **374**, 453–457 (1995).

62. Pi, J. S. *et al.* The olivary input to the cerebellum dissociates sensory events from movement plans. *Proc. Natl. Acad. Sci.* **121**, e2318849121 (2024).

63. Thach, W. T. Somatosensory receptive fields of single units in cat cerebellar cortex. *J. Neurophysiol.* **30**, 675–696 (1967).

64. Sato, Y., Miura, A., Fushiki, H. & Kawasaki, T. Short-term modulation of cerebellar Purkinje cell activity after spontaneous climbing fiber input. *J. Neurophysiol.* **68**, 2051–2062 (1992).

65. Romano, V. *et al.* Olivocerebellar control of movement symmetry. *Curr. Biol.* **32**, 654-670.e4 (2022).

66. Streng, M. L., Popa, L. S. & Ebner, T. J. Climbing Fibers Control Purkinje Cell Representations of Behavior. *J. Neurosci.* **37**, 1997–2009 (2017).

67. Siegle, J. H. *et al.* Open Ephys: an open-source, plugin-based platform for multichannel electrophysiology. *J. Neural Eng.* **14**, 045003 (2017).

68. Sedaghat-Nejad, E. *et al.* P-sort: an open-source software for cerebellar neurophysiology. *J. Neurophysiol.* **126**, 1055–1075 (2021).

69. Pachitariu, M., Steinmetz, N., Kadir, S., Carandini, M. & D, H. K. Kilosort: realtime spike-sorting for extracellular electrophysiology with hundreds of channels. 061481 Preprint at https://doi.org/10.1101/061481 (2016).

70. Hage, P. *et al.* Effort cost of harvest affects decisions and movement vigor of marmosets during foraging. *eLife* **12**, (2023).

71. Kojima, Y., Robinson, F. R. & Soetedjo, R. Cerebellar fastigial nucleus influence on ipsilateral abducens activity during saccades. *J. Neurophysiol.* **111**, 1553–1563 (2014).

72. Bourrelly, C., Quinet, J. & Goffart, L. The caudal fastigial nucleus and the steering of saccades toward a moving visual target. *J. Neurophysiol.* **120**, 421–438 (2018).

73. Becker, M. I. & Person, A. L. Cerebellar Control of Reach Kinematics for Endpoint Precision. *Neuron* **103**, 335–348 (2019).

74. Muller, S. Z. *et al.* Complex spikes perturb movements and reveal the sensorimotor map of Purkinje cells. *Curr. Biol.* **33**, 4869-4879.e3 (2023).

75. Ruigrok, T. J. H. & Voogd, J. Organization of projections from the inferior olive to the cerebellar nuclei in the rat. *J. Comp. Neurol.* **426**, 209–228 (2000).

76. Apps, R. & Garwicz, M. Anatomical and physiological foundations of cerebellar information processing. *Nat.Rev.Neurosci.* **6**, 297–311 (2005).

77. Welsh, J. P., Lang, E. J., Suglhara, I. & Llinas, R. Dynamic organization of motor control within the olivocerebellar system. *Nature* **374**, 453–457 (1995).

78. Hoogland, T. M., De Gruijl, J. R., Witter, L., Canto, C. B. & De Zeeuw, C. I. Role of Synchronous Activation of Cerebellar Purkinje Cell Ensembles in Multi-joint Movement Control. *Curr. Biol.* **25**, 1157–1165 (2015).

79. Kitazawa, S., Kimura, T. & Yin, P. B. Cerebellar complex spikes encode both destinations and errors in arm movements. *Nature* **392**, 494 (1998).

80. Hewitt, A. L., Popa, L. S. & Ebner, T. J. Changes in Purkinje cell simple spike encoding of reach kinematics during adaption to a mechanical perturbation. *J.Neurosci.* **35**, 1106–1124 (2015).
81. Heffley, W. *et al.* Coordinated cerebellar climbing fiber activity signals learned sensorimotor predictions. *Nat. Neurosci.* **21**, 1431–1441 (2018).
82. Wagner, M. J. *et al.* A neural circuit state change underlying skilled movements. *Cell* **184**, 3731-3747.e21 (2021).
83. Calame, D. J., Becker, M. I. & Person, A. L. Cerebellar associative learning underlies skilled reach adaptation. *Nat. Neurosci.* 1–12 (2023) doi:10.1038/s41593-023-01347-y.
84. Ishikawa, T. *et al.* Releasing dentate nucleus cells from Purkinje cell inhibition generates output from the cerebrocerebellum. *PLoS.One.* **9**, e108774 (2014).
85. Pi, J. S. *et al.* The olivary input to the cerebellum dissociates sensory events from movement plans. *Proc. Natl. Acad. Sci.* **121**, e2318849121 (2024).
86. Kojima, Y. & Soetedjo, R. Elimination of the error signal in the superior colliculus impairs saccade motor learning. *Proc.Natl.Acad.Sci.U.S.A* **115**, E8987–E8995 (2018).
87. Kojima, Y. & Soetedjo, R. Change in sensitivity to visual error in superior colliculus during saccade adaptation. *Sci.Rep.* **7**, 9566 (2017).
88. May, P. J., Warren, S. & Kojima, Y. The Superior Colliculus Projection Upon the Macaque Inferior Olive. https://www.researchsquare.com (2023) doi:10.21203/rs.3.rs-2986616/v1.
89. Soetedjo, R., Kojima, Y. & Fuchs, A. F. How cerebellar motor learning keeps saccades accurate. *J. Neurophysiol.* **121**, 2153–2162 (2019).
90. Gao, Z. *et al.* A cortico-cerebellar loop for motor planning. *Nature* **563**, 113–116 (2018).
91. Chabrol, F. P., Blot, A. & Mrsic-Flogel, T. D. Cerebellar Contribution to Preparatory Activity in Motor Neocortex. *Neuron* **103**, 506–519 (2019).

92. Zhu, J., Hasanbegović, H., Liu, L. D., Gao, Z. & Li, N. Activity map of a cortico-cerebellar loop underlying motor planning. *Nat. Neurosci.* 1–13 (2023) doi:10.1038/s41593-023-01453-x.

93. Herzfeld, D. J., Kojima, Y., Soetedjo, R. & Shadmehr, R. Encoding of error and learning to correct that error by the Purkinje cells of the cerebellum. *Nat.Neurosci.* **21**, 736–743 (2018).

Chapter 6 Curriculum Vitae

Paul Hage

CONTACT INFORMATION

Laboratory for Computational Motor Control, Johns Hopkins University

720 Rutland Ave, 416 Traylor Building, Baltimore, MD 21205.

E-mail: paulhage253@gmail.com

EDUCATION

Ph.D., Biomedical Engineering *Aug 2018 – June 2024*

Johns Hopkins School of Medicine (JHU), Baltimore, Maryland, USA

- Area of study: Systems Neuroscience and Neuroengineering
- Thesis: Neural control of the tongue in the common marmoset
- Mentor: Professor Reza Shadmehr

B.Sc., Electrical Engineering *Sep 2015 – Dec 2017*

University of Washington (UW), Bothell, Washington, USA

LEADERSHIP ROLES

- **Primary Co-Investigator** of protocol PR16M381, *Cerebellar correlates of motor learning in the marmoset monkey*, Principal Investigator: Dr. Reza Shadmehr, JHU. *July 2022 – June 2024*.

SELECTED AWARDS

- President's Medal, UW. *2018.*
- Mary Gates Research Scholar, Mary Gates Endowment. *2016.*
- NASA Space Grant Research Scholar, NASA Washington Space Grant Consortium. *2016.*

TEACHING EXPERIENCES

- Lead teaching assistant for "Principles of Design of BME Instrumentation", Instructor Dr. Nitish Thakor, JHU. *Fall 2022.*

PEER REVIEWED JOURNAL PUBLICATIONS

- Shoup, A. M., Porwal, N., Fakharian, M. A., **Hage, P.**, Orozco, S. P., & Shadmehr, R. (2024). Rejuvenating silicon probes for acute electrophysiology. ***Journal of Neurophysiology***, 1522-1598.
- Pi, J. S., Fakharian, M. A., **Hage, P.**, Sedaghat-Nejad, E., Muller, S. Z., & Shadmehr, R. (2024). The olivary input to the cerebellum dissociates sensory events from movement plans. ***Proceedings of the National Academy of Sciences*** *of the United States of America*, 121 (17), e2318849121.
- **Hage, P.**, Jang, I. K., Looi, V., Fakharian, M. A., Orozco, S. P., Pi, J. S., Sedaghat-Nejad, E., & Shadmehr, R. (2023). Effort cost of harvest affects decisions and movement vigor of marmosets during foraging. ***eLife***, 12: RP87238.
- Muller*, S. Z., Pi*, J. S., **Hage, P.**, Fakharian, M. A., Sedaghat-Nejad, E., & Shadmehr, R. (2023). Complex spikes perturb movements and reveal the sensorimotor map of Purkinje cells. ***Current Biology***, 33(22), 4869–4879. (*equal contribution)
- Sedaghat-Nejad, E., Pi, J.S., **Hage, P.**, Fakharian, M.A., & Shadmehr, R. (2021). Synchronous spiking of cerebellar Purkinje cells during control of movements. ***Proceedings of the National Academy of Sciences*** *of the United States of America*, 119(14), e2118954119.
- Sedaghat-Nejad, E., Fakharian, M.A., Pi, J.S., **Hage, P.**, Kojima, Y., Soetedjo, R., Ohmae, Sh., Medina, J., & Shadmehr, R. (2021). P-sort: an open-source software for cerebellar neurophysiology. ***Journal of Neurophysiology***, 126(4), 1055–1075.
- Sedaghat-Nejad, E., Herzfeld*, D.J., **Hage*, P.**, Karbasi, K., Palin, T., Wang, X., & Shadmehr, R. (2019). Behavioral training of marmosets and electrophysiological recording from the cerebellum. ***Journal of Neurophysiology***, *122(4)*, 1502–1517. (*equal contribution)
- Roychowdhury, S., **Hage, P.**, & Vasquez, J. (2017). Azure-based smart monitoring system for anemia-like pallor. ***Future Internet***, *9*(3), 39.

PEER REVIEWED CONFERENCE PROCEEDINGS

- Pi, J.S., Fakharian, M.A., **Hage, P.**, Sedaghat-Nejad, E., Muller, S. Z., & Shadmehr, R. (2023). Complex spikes independently encode sensory prediction errors and movements. ***Proceedings of Advances in Motor Learning and Motor Control***.
- **Hage, P.**, Jang, I. K., Looi, V., Fakharian, M. A., Orozco, S. P., Pi, J. S., Sedaghat-Nejad, E., & Shadmehr, R. (2022). Effects of reward and effort on decision-making and movement vigor of marmosets. ***Proceedings of Advances in Motor Learning and Motor Control***
- Sedaghat-Nejad, E., Pi, J.S., **Hage, P.**, Fakharian, M.A., & Shadmehr, R. (2021). Synchronous spiking of cerebellar Purkinje cells during control of movements. ***Proceedings of Advances in Motor Learning and Motor Control***.
- Sedaghat-Nejad, E., **Hage, P.**, Pi, J., Shadmehr, R. (2020). Population coding of saccadic eye movements by Purkinje cells of the marmoset cerebellum. ***Proceedings of Advances in Motor Learning and Motor Control***.
- Roychowdhury, S., Sun, D., Bihis, M., Ren, J., **Hage, P.**, & Rahman, H. H. (2017). Computer aided detection of anemia-like pallor. *2017 IEEE EMBS International Conference on Biomedical & Health Informatics,* 978-1-5090-4179-4.

INVITED TALKS

- Effort cost of harvest affects decisions and movement vigor of marmosets during foraging. (2024). Invited talk at: *Japan Society for Marmoset Research*.
- Effort cost of harvest affects decisions and movement vigor of marmosets during foraging. (2023). Invited talk at: *JHU Cerebellum Seminar.*
- Effects of reward and effort on decision-making and movement vigor of marmosets. (2023). Invited talk at: *Advances in Motor Learning and Motor Control*.
- Investigating the role of Purkinje cells in control of the marmoset tongue. (2020). Invited talk at: *Dr. Zee's Ocular Motor and Vestibular Lecture Series.*
- Electrophysiological recording from the marmoset cerebellum. (2020). Invited talk at: